Journal of Engineering and Technology
of the Open University of Sri Lanka

Volume 04 No. 02 September 2016 ISSN 2279-2627

All correspondence should be addressed to:

Editor in Chief- Journal of Engineering and Technology
Faculty of Engineering Technology
The Open University of Sri Lanka
Nawala, Nugegoda
Sri Lanka
Email: meper@ou.ac.lk, Telephone: +94112881061

The Journal of engineering and technology of the Open University of Sri Lanka is a peer-reviewed journal published bi-annually by the Faculty of Engineering Technology of the Open University of Sri Lanka. The Journal accepts original articles based on theoretical and applied research in the area of Engineering and Technology in all specializations.

CONTENTS

Volume 04 No. 02 September 2016 ISSN 2279-2627

Page

Optical Sensor to Detect Titration End Point to Evaluate Hardness of Drinking Water

S.A.D.A.N Dissanayake[1*], H. Pasqual[1], B. C. L. Athapattu[2]

[1]Department of Electrical and Computer Engineering, The Open University of Sri Lanka, Nawala, Nugegoda, Sri Lanka.

[2]Department of Civil Engineering, The Open University of Sri Lanka, Nawala, Nugegoda, Sri Lanka

Corresponding Author: email: sadis@ou.ac.lk, Tele: +94112881272

Abstract – *Complexometric titration is a commonly used method to test hardness of water. Since small variation of colour is non observable to the naked eye in colorimetric method, it is advisable to use a sensor to monitor the variation of the signal throughout the titration process, which helps to detect the correct end point of the process. This paper discusses the ability of finding end point of titration using colorimetric method. Beer Lambert law was used for computing colour absorbance of the optical sensor. Three colours were transmitted via a solution one at a time, to detect the end point accurately. Less volumes of sample and titrant make an environmental friendly approach. The developed sensor is capable of detecting concentration of hardness from 100 mg/L to 1000 mg/L and automation of the device allows the process with no expert involvement.*

Keywords: *Colorimetric method, Titration end point, hardness, optical sensor*

Nomenclature

A - Absorbance
ε - Molar absorptivity (L $mol^{-1}cm^{-1}$)
c- Concentration of the compound in solution (mg/L)
l - Solution path length (cm)
P_{in} - Intensity of the light source (W/m^3)
P_{out} - Intensity to the light detector (W/m^3)

1 INTRODUCTION

Measurement of hardness of water is important though there are fewer health hazards. However, long term consumption can lead to diseases such as nephrolithiasis (kidney stones), colorectal cancer, hypertension and stroke, coronary artery disease, insulin resistance (USGS 2016). Hardness in water causes to precipitate calcium and magnesium in boilers, kettles. However, long term consumption of such water directly impact on human health. According to many researchers (Chandrajith *et al.*. 2011; Dharmawardana

et al. 2014; Jayasumana *et al.* 2014), hardness is one of a supporting ingredient to produce complexes that cause the Chronic Kidney Diseases of Unknown etiology (CKDu). Dharmawardana *et al.* (2014) explain the possibility of drinking high ionicity of water effects on the kidney function. Apart from that the ground water used for drinking and domestic purposes may have unique fluoride, sodium and calcium ion concentrations, which could also be led to make complexities on fatal chronic kidney diseases (Chandrajith *et al.* 2011). The degree of hardness of drinking water has been classified in terms of the equivalent $CaCO_3$ concentration as shown in table 1. The SLSI 614:2013 standard of potable water recommends that the permissible level of hardness is 250mg/L, which implies that more than the said concentration is not suitable for drinking.

Table 1: Classification of hard water according to the $CaCO_3$ concentration

Classification	Hardness levels
Soft	0-60mg/L
Medium	60-120mg/L
Hard	120-180mg/L
Very Hard	>180mg/L

Note. From USGS Water-Quality Information, May 2016

The laboratory and portable instruments used for detection of hardness need skilled person to operate the instrument. Even with the presence of a skilled person, small variation of colour cannot be identified with the naked eye. The end titration point will change the reading of the concentration of ions. Therefore, this paper proposes a design of sensor for detection of hardness. The developed sensor will be embedded into an instrument enabling to obtain direct reading and minimize the cost as well as the time taken for the delivery of the samples to the laboratory.

2 REVIEW OF LITERATURE

Optical sensing can be used for many purposes. Omar *et al.* (2008) and Daraigan *et al.* (2007) illustrate a mechanism to calculate total suspended solids (TSS) in water. Transmittance and 90 degree scattering technique is used to evaluate the water quality of the system in Omar *et al.* (2008). This system consists of optical sensor with a fiber optic cable as the transmission media which is used in an experimental setup to evaluate the turbidity of water. The results has been obtained by emitting two wave lengths, 470nm (BLUE system) and 635 nm (RED system) tested with a known clay concentration for turbidity. Nitrate, sodium, calcium ions and heavy metal concentrations can be identified using electrodes and optrodes according to the studies carried out by Hanrahan *et al.* (2004), Thompson *et al.* (2014) and Pereira *et al.* (2007). Hanrahan *et al.* (2004) explains the

use of electrodes as the sensing element for environmental monitoring. There are various types of commercially available ion-selective electrodes such as Ca^{2+}, Ba^{2+}, Pb^{2+}, Zn^{2+}, Cd^{2+}, Mg^{2+}, Cs^{+}, NH_4^{+}, Ag^{+}, Na^{+} etc. Ion Selective Optrode System (ISOS) of Thompson *et al.* (2014) is capable of identifying the ion concentration of K^{+}, Na^{+}, Ca^{2+}, and NO^{3-} separately. The optrode, the sensing element consists of a Light Emitting Diode (LED) as an optical source, ion selective optrode film which produces the measurement of the ion concentration of a solution in the form of a colour change through spectrometer. Winkler (Furuya&Harada, 1995) and Karl Fischer (Koch *et al.* 2007) titrations are used to measure moisture content and dissolve oxygen respectively.

Complexometric titration, potentiometric titration, Atomic Absorption Spectrometry (AAS), Ion Selective Electrode (ISE) and optical test strips are few analyzing methods to detect concentration of hard water. Vahal *et al.* (2010) explains potentiometric detection via flow injection analysis (FIA) titrations to determine the Calcium and Magnesium in aqueous solutions. System is capable of determining pH value along with the hardness measurement. Optical test strip described in Capitán-Vallvey *et al.* (2003) uses ion exchange chromatography to detect the hardness of water. Life span of the optical test strip is one and half months when protected from the light. Paull *et al.* (1997) used graphitic as the stationary phase and o-cresolphthaleincomplexone as the mobile phase to separate ions in order to measure ion concentration through liquid chromatography. Filik *et al.* (2011) show that low concentration of calcium in water and milk can be identified by reflectance spectroscopy.

In laboratories the hardness is measured using Ethylenediaminetetraacetic acid (EDTA) solution with the Erichrome Black T indicator by detecting colour change in the solution. EDTA forms colour complexes with metal ions (Manahan, 1994). At pH 10, calcium and magnesium ions indicate colour change from red wine to blue in the absence of Ca^{++} and Mg^{++} ions as they make complexes using ionic Ca^{++} and Mg^{++}in the sample. This scenario was used in detecting the concentration of calcium and magnesium ions in colorimetric instruments. Bhattacharjee *et al.* (2013) has developed a sensor for detecting hardness using colorimetric concept. They captured colour change from red wine to blue through a photo detector, which gives appropriate titration point though voltage variation. In their study voltage variation of blue and red were 13% and 74% respectively. This paper presents the development of optical sensor to detect the end point of complexometric titration using three colours with further accuracy.

3 THEORY

Optical intensity was used as the sensing mechanism to detect the colour variation of the titration point. Absorption is defined as negative logarithmic of the transmittance as in equation (1).

$$A = -\log\left[\frac{P_{out}}{P_{in}}\right] \tag{1}$$

Incident power (P) is proportional to the photocurrent (I_p) of the detector as in equation

(2). Responsivity (R) is the proportional constant for a given range of wavelengths.

$$P = RI_p \tag{2}$$

Substituting the photo current which generated without solution ($I_{p\ (in)}$) and the photocurrent which generated after passing through the solution ($I_{p\ (out)}$) in equation (2), Absorption of the solution for a particular wavelength,

$$A = \log\left[\frac{RI_{p(in)}}{RI_{p(out)}}\right]$$

$$A = \log\left[\frac{I_{p(in)}}{I_{p(out)}}\right] \tag{3}$$

Beer – Lambert's law states that,

$$A=\varepsilon cl \tag{4}$$

Hence,

$$c = \frac{1}{\varepsilon l} \times \log\left[\frac{I_{p(in)}}{I_{p(out)}}\right] \tag{5}$$

According to the equation (5), generated current in the detector associates with concentration of an analyte in a solution. Also the reflection, scattering, refraction through the medium has to be minimized to obtain the linear relationship of logarithmic of the photocurrent variation to the concentration of the analyte.

Variations of photocurrent due to colours (or wavelengths) are used for detection of the titration point. Details of the detection mechanism is described in section 4.2.

4 METHODOLOGY

4.1 Reagents and standard solutions

Weight of 3.723g analytical grade disodium ethylene diamine tetra acetate dehydrate (also known as disodium salt of EDTA) was dissolved with 1000ml deionized water to prepare EDTA 0.01 M solution. pH 10 buffer was prepared dissolving 16.9g ammonium chloride with 143ml conc. ammonia and top up the solution to 250 ml with deionized water. Erichrome black T powder (Sodium salt of 1 - (1- hydroxyl - 2 -naphthylazo) - 5 - nitro - 2 - naphthol - 4 - sulfonic acid) indicator was prepared by grinding 0.2g indicator with 50g KCl and stored in a dark colour bottle.

In order to prepare the standard calcium solution (1ml = 1.00mg $CaCO_3$), weighted 1.000g anhydrous $CaCO_3$ is mixed with 1+1 HCl to dissolve $CaCO_3$. 200ml of de ionized water was added and boiled for few minutes and left the solution to cool. Few drops of methyl red indicator was added to develop slight orange colour by adding 3N NH_4OH or 1+1 HCl as required. Prepared quantity was diluted to 1000ml with de ionized water (APHA 2005).

4.2 System methodology

Sensor consists of red, blue, and orange (absorption colour of blue) colour LEDs and phototransistors to detect colour intensity. In the tested set up, plastic cuvette was used to keep the solution in between LEDs and phototransistors. 5 ml of sample water, 0.2 ml of buffer solution (pH 10) and Eriochrome Black T powder were added and mixed to get cherry red /purple colour. Then EDTA solution was added and voltage variation was observed to check the end point of the titration which gives a blue colour.

Addition of EDTA was continued till the colour variation of red wine to blue indicates at the detector. End point of the titration was detected at the point where the voltage drops with orange and red colour lights and rises with blue colour light. When the detector identifies the blue colour the process was stopped and the amount of used volume of EDTA solution was measured for the calculation.

Total hardness is calculated using equation (6) (APHA,2005).

$$Hardness\ (EDTA)\ as\ mg\ CaCO_3/L = \frac{P \times Q \times 1000}{mlSample} \quad (6)$$

where:

P= ml titration for sample

Q = mg $CaCO_3$ equivalent to 1.00 ml EDTA titrant.

$CaCO_3$ equivalent to 1.00ml EDTA titrant (Q) was estimated by titrating 25 ml known concentration (1000mg/L) of $CaCO_3$ solution with 25 ml of EDTA solution. Using Equation (6), Q was computed as 1.

4.3 Reference Methodology

EDTA titration method was used to detect the total hardness of water samples. APHA (2005) testing procedure was adopted as the reference methodology. 25 ml of sample was mixed with deionized water to have a volume of 50 ml of sample for testing. This has been used to check the accuracy of the developed optical sensor.

4.4 Preparation for testing water samples

The buffer solution was added to the sample to be tested until the pH of the sample becomes 10. The 0.5 ml of EBT was added to the sample in order to develop wine red colour. The colour developed sample was used for titration to detect the end point.

5 RESULTS AND DISSCUSSION

5.1 Validation of optical sensor

Small photocurrent variation needs to be analyzed to detect the endpoint. Even though the endpoint can be detected with a single colour variation, with small voltage variations it is difficult to identify the exact end point. Bhattacharjee *et al*. (2013) used two colour LEDs (red and blue) to detect the titration end point. Analysis of multiple signal variation patterns can be used to detect the exact end point further accurately. Accordingly absorbing colour of blue, which is orange was used to check the accuracy of the titration end point.

Optical sensor was tested with the standard solution (1000 mg/L) and the test results are tabulated in Table 2.

Table 2: Voltage variations of three colours with the added EDTA titrant volume with the standard solution

EDTA titrant (ml)	V(Orange)	V(Red)	V(Blue)
0ml (EDTA)	14.5	445	66.7
1ml (EDTA)+	17.1	472	91.1
1ml (EDTA)+	19.2	503	112.8
1ml (EDTA)+	21.3	515	138
1ml (EDTA)+	22.3	512	158.5
0.2ml (EDTA)+	23.5	490	159.3
0.3ml (EDTA)+	22.5	0.451	163.3
0.2ml (EDTA)+	20.1	0.362	174.8
0.3ml (EDTA)+	11.6	0.141	215.6
0.2ml (EDTA)+	10	0.114	210.8

At the beginning the voltages of three colours, increase with the addition of EDTA. A slight drop of the voltages of red and orange light was noted, in the instance of adding 4.5 ml of EDTA. A clear voltage difference was observed at the next drop of EDTA. The titration point was occurred at the point where 5 ml of EDTA added. Value of Q in equation (6) was computed as 1. The results revealed that the Q computed using developed optical sensor is similar to the reference method.

5.2 Testing water samples

Five water samples from Anuradhapura district were tested using the developed sensor. Tables 3 -7, present voltage readings of phototransistor according to the colour of the LED. Titration point was selected as described in section 4.2.

Table 3: Voltage variations of three colours with the added EDTA titrant volume with water sample 1

EDTA titrant (ml)	Output voltage (mV)		
	V(Orange)	V(Red)	V(Blue)
0ml (EDTA)	10.4	304	32.9
0.5ml (EDTA)+	8.8	248	25.1
0.5ml (EDTA)+	9.4	250	29.7
0.3ml (EDTA)+	8.6	195	34.2
0.3ml (EDTA)+	1.8	2.1	54.1

According to the data in table 3, sample 1 consumed 1.6ml of EDTA solution. The hardness of sample 1 was computed using equation (6) resulted as 320 mg/L. Similarly

hardness of sample 2, which consumed 1.8 ml of EDTA solution was estimated as 360mg/L. Highest variation of the voltage captured was in blue light in sample 2 that supports to detect exact titration end point.

Table 4: Voltage variations of three colours with the added EDTA titrant volume with water sample 2

EDTA titrant (ml)	Output voltage (mV)		
	V(Orange)	V(Red)	V(Blue)
0ml (EDTA)	11.9	322	46.2
0.5ml (EDTA)+	12.8	305	47.4
0.5ml (EDTA)+	13.3	308	53.8
0.3ml (EDTA)+	13.3	271	56.8
0.2ml (EDTA)+	9	149	68.8
0.1ml (EDTA)+	9	125	131.3

Table 5: Voltage variations of three colours with the added EDTA titrant volume with water sample 3

EDTA titrant (ml)	Output voltage (mV)		
	V(Orange)	V(Red)	V(Blue)
0ml (EDTA)	4.5	157	13.1
0.2ml (EDTA)+	3.4	88	9.4
0.2ml (EDTA)+	4.4	101	14.5
0.3ml (EDTA)+	4	88.5	15.8
0.1ml (EDTA)+	1.8	3.5	26

Hardness of sample 3 is low compared to other samples, which was calculated as 160 mg/L consumed 0.8 ml of EDTA solution. Red colour indicated the significant voltage variation to identify the endpoint of the titration.

Table 6: Voltage variations of three colours with the added EDTA titrant volume with water sample 4

EDTA titrant (ml)	Output voltage (mV)		
	V(Orange)	V(Red)	V(Blue)
0ml (EDTA)	18.6	445	80.5
0.5ml (EDTA)+	14.9	390	68
0.5ml (EDTA)+	16.8	390	78.6
0.3ml (EDTA)+	16.9	391	92.2
0.1ml (EDTA)+	14.4	270	97
0.1ml (EDTA)+	4.9	35	125.9

Sample 4 consumed 1.5 ml of EDTA solution and calculated hardness was 300 mg/L. Voltage variations of all colours were significant and supported the decision.

Table 7: Voltage variations of three colours with the added EDTA titrant volume with water sample 5

EDTA titrant (ml)	Output voltage (mV)		
	V(orange)	V(Red)	V(Blue)
0ml (EDTA)	11.4	333	25.3
0.5ml (EDTA)+	8.1	233	26.4
0.4ml (EDTA)+	8.9	220	27.5
0.3ml (EDTA)+	5.5	83.4	35.5

Sample 5 consumed 1.6 ml of EDTA solution which was used to calculate hardness of 240 mg/L. Voltage variation of the orange colour was not obeyed the variation properly at the beginning. Therefore blue and red supported to take the decision correctly for sample 5.

In the present study, calculated hardness using designed optical sensor of five samples were compared with APHA standard for hardness detection and summarized in Table 8. Samples 1, 2 and 5 were deviated from around 10%, 12% and 5% respectively. 100% accuracy was achieved by the two samples compared to the standard solution measurements. This indicates that the accuracy can be increased adding small drops of EDTA solution at a time. Testing was done manually to check the sensor responses.

In the sensor developed by Bhattacharjee *et al*. (2013) the error variations of red light voltage readings differ around 74%, while blue which is around 13%. In the present study, three colour optical sensor showed higher accuracy compared to the two colour optical sensor.

Table 8: Comparison of sensor design with the APHA standard procedure for hardness detection

Sample	Hardness (mg/L)	
	Designed sensor	APHA standard
1	320	372
2	360	404
3	160	160
4	300	300
5	240	252

Fig.1 shows the comparison of consumption EDTA volume in the designed setup and reference method. Contrast with the referenced procedure it shows a reduction of 20% of EDTA volume for a sample. As the sample size reduced the wastage also reduces. This is helpful in managing waste as the processors of recycles also cost money.

The sensor was closed and covered with a black casing to reduce the reflections within the unit and the influence of the environment light effects. Error variations are due to the manual testing of the sensor and it can be overcome when the sensor is automated in near future. The developed optical sensor measures hardness levels from 100 to 1000 mg/L, which generally indicates at the CKDu prevalence areas. Summary of the work shows that the developed sensor is in working condition and the testing is in progress for the improvements.

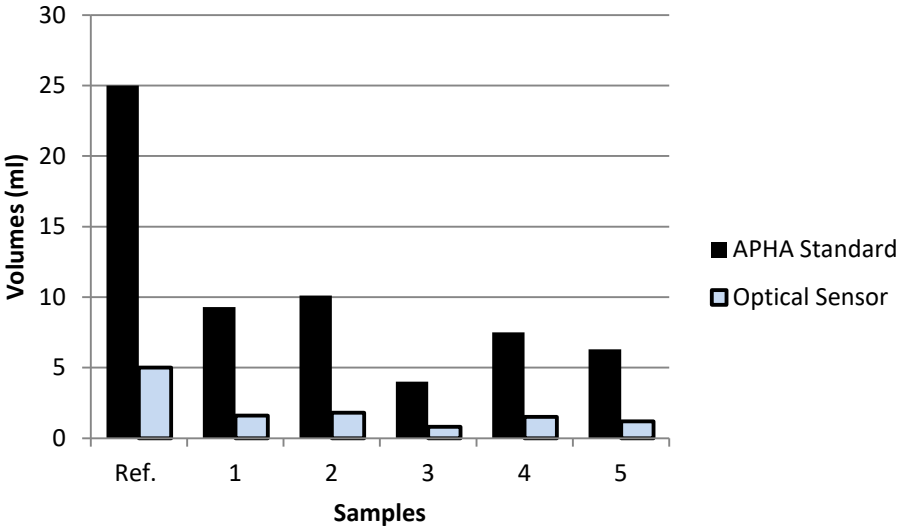

Figure 1: Volumes of EDTA consume in each sample with APHA standard procedure and optical sensor procedure

6 CONCLUSIONS / RECOMMENDATIONS

Three colour optical sensor is a successful method to detect titration end point to evaluate hardness of drinking water accurately. Hardness levels from 100 to 1000 mg/L can be measured using the designed sensor. Compared with the reference methodology the sample volume, EDTA volume and EBT powder consumption are reduced which makes an eco friendly approach. The low power consumption of the detector helps to use the sensor for a longer period of time. Improving user friendliness of the developed sensor through automation is under investigation. Automated system will help to test the water and advise the community whether to avoid or filter the water before drinking.

7 ACKNOWLEDGEMENT

The authors are thankful to Dept. of Agricultural and Plantation Engineering, Dept. of Civil Engineering, Dept. of Chemistry, Dept. of Electrical and Computer Engineering and National Water Supply and Drainage Board, regional support center, Anuradhapura for supporting this study and University Research Fund of The Open University of Sri Lanka for the financial support.

REFERENCES

1. APHA, (2005).Standard methods for the Examinations of Water and Wastewater, 2st ed. American Public Health Association, Washington, D.C.

2. Bhattacharjee, T., Jiang, H.,Behdad, N.(2013) Sensor Design for Water Hardness Detection, SENSORS IEEE,1-4.

3. Capitán-Vallvey, L.F., Fernández-Ramos, M.D., Gálvez, P. A. de C&Santoyo-González, F.(2003). Characterisation of a transparent optical test strip for quantification of water hardness.AnalyticaChimica Acta,481,139–148.

4. Chandrajith R, Dissanayake C.B, ThivankaAriyarathna, Herath H.M.J.M.K, Padmasiri J.P, (2011) Dose-dependent Na and Ca in fluoride-rich drinking water - Another major cause of chronic renal failure in tropical arid regions, Science of the Total Environment, 671–675.

5. DaraiganS.G, Hashim S.A, Mohd.Jafri Z.M, Abdullah K, Jeng W.C and NasirunMohd.Saleh, (2007) Multispectral Absorption Algorithm for retrieving TSS concentrations in water, Geoscience and Remote Sensing Symposium, 2848 – 2851.

6. Dharmawardaha M.W.C *et al.* (2014) Chronic Kidney Disease of Unknown aetiology and ground-water ionicity; study based on Sri Lanka, Environmental Geochemistry and Health, Available at http://link.springer.com/journal/10653

7. Furuya K andHarada K (1995) An Automated Precise Winkler Titration for Determining, Dissolved Oxygen on Board Ship, Journal of Oceanography,51, 375 - 383.

8. Filik H, Aksu D, Apak R, (2011) Rapid Determination of Calcium in Milk and Water Samples by Reflectance Spectroscopy, American Journal of Analytical Chemistry, 2, 276-283

9. Hanrahan G, Patila D.G. and Wang J, (2004) Electrochemical sensors for environmental monitoring: design,development and applications, J. Environ. Monit., 6, 657 -664.

10. Jayasumana C, Gunathilake S, Senanayake P, (2014), Glyphosate, Hard water and Nephrotoxic Metals: Are they the culprits Behind the Epidemic of Chronic Kidney Disease of Unknown etiology in Sri Lanka, International Journal of Environmental Research and Public Health, pages 2125 – 2147.

11. Koch M, Tenbohlen S, Blennow J, HoehleinI (2007) Reliability and Improvements of Water Titration by the Karl Fischer Technique, Retrieved from: https://www.researchgate.net/profile/Stefan_Tenbohlen/publication/268395208_Reliability_and_Improvements_of_Water_Titration_by_the_Karl_Fischer_Technique/links/54d34a520cf250179181df87.pdf

12. Manahan S.E, (1994)Environmental Chemistry, United States of America, Lewis.
Omar A.F, MatJafri M.Z ,Water Quality Measurement using transmittance and 90°

Scattering Techniques through optical fiber sensor', NCTT-MCP 2008. 6th National Conference, Putrajaya, pp: 17 – 21.

13. Paull,B.,Macka,M.&Haddad,P.R.(1997).Determination of calcium and magnesium in water samples by high-performance liquid chromatography on a graphitic stationary phase with a mobile phase containing o-cresolphthaleincomplexone,Journal of Chromatography A,789,329–337.

14. Pereira J.M.D, Postolache O, Girao P.S (2007)A Smart and Portable solution for Heavy Metals concentration Measurements, IMTC Warsaw, Poland, pp:1-4

15. Thompson C.G, Sobron P, Dixon M. A, Cabrol N. and the 2013 PLL Team CESRF University of Guelph, Using Ion-Selective Optrodes to Characterize water chemistry in extreme environment, 2014, 45th Lunar and Planetary Science Conference, Retrieved from http://www.hou.usra.edu /meetings/ lpsc2014 /pdf/2205.pdf

16. Vahal, K., Kahlert, H.&Scholz, F.(2010).Rapid Atomatic Determination of Clacium and Magnesium in Aqueous Solutions by FIA using Potentiometric Detection, Electroanalysis,19,2172 – 2178.

Wheel Speed Control Algorithm for Rear Wheel Motor Driven Vehicle

D.C. Hewage[1], I.A. Premaratne[2*]

[1]Network Operation Centre, Etisalat Lanka LTD,
Rotunda Gardens, Colombo 3, Sri Lanka

[2]Department of Electrical and Computer Engineering, The Open University of Sri Lanka, Nawala, Nugegoda, Sri Lanka

*Corresponding Author: email: iapre@ou.ac.lk, Tele: +94112881272

Abstract – *The conventional vehicles in the past had consisted of mechanical differential which converts the engine torque in to two directions. Due to the introduction of electric vehicle the vehicle propulsion system has changed from combustion engine to electric motor. Since the concept of differential is a must have component to drive a vehicle, it is still used in electric vehicles as well. Common method is a motor generates the torque and transmit it to the wheels through a mechanical differential. It is possible to connect two small motors to each wheel rather than making a large motor and connects a mechanical differential. In order to drive two motors independently it is required to set the correct speeds when the vehicle takes a turn. This research has been conducted to find a control algorithm using a mathematical model to set the ratio of wheel speeds of inner and outer wheels to make a smooth turn while maintaining the desired speed of linear motion. The algorithm has been tested using a prototype model and proved the calculation of wheel speed ratio and actual scenario.*

Keywords: *Control Algorithm, Electric Vehicle, Electronic Differential, Mathematical Model*

Nomenclature

EV -Electric vehicle
GUI – Graphical user interface
V - Linear speed
PID - proportional–integral–derivative
PWM – Pulse width modulated
RPM - Revolutions per minute
R_d – Radius of the wheel
V_{read}– Linear speed measurement
V_{Rread} – Right wheel measuredspeed
V_{Lread}– Left wheel measured speed
V_L – Left wheel set speed
V_R– Right wheel set speed

Greek Letters
ω - Angular velocity

Subscripts
inner-inside of bend
outer-outside of bend
read – measured value

1 INTRODUCTION

Electric vehicles are the latest trend in automobile industry. As per the decay of fossil fuel resources in the world, the automobile manufacturers attempted on manufacturing electric vehicles (EV). These are powered by internal battery and the propulsion system is electric motor. Due to the increment of electronic components in vehicles, several electronic control systems such as automatic parking guidance, dynamic breaking and energy controlling are installed in these vehicles. This area has rapid outcomes with the introduction of new technology to the market.

The differential is a device which splits the engine torque in to two ways, allowing each output to spin at a different speed. When the vehicle takes a turn, the inner wheels rotate at a lower speed than the outer wheels. This concept is clearly explained in the next section of this paper. The differential is found in all vehicles including rear-wheel, front-wheel and all-wheel-drive vehicles. This component individually controls the outer and inner wheels of the vehicle and let the vehicle take a turn properly. Conventional differential is a mechanical component and this has been assembling in vehicles for decades. Still almost all the commercial vehicles employ the conventional mechanical differential. Electronic differential is an innovative concept in electric vehicle technology research areas. In here, wheels are powered by individual motors and the electronic controlling performs the functionality of the differential. There are many advantages by using an electronic controlled differential in a vehicle.

The objective of this research is to develop a control algorithm for an electronic differential. This paper will illustrate the concept of electronic differential, discuss the advantages compared to conventional differential and discuss future improvements. A mathematical model is developed to validate the input-output relationship of the algorithm. The algorithm is simulated and tested with a prototype model.

2 ADVANTAGES OF ELECTRONIC CONTROL SYSTEMS OVER MECHANICAL CONTROL SYSTEMS

Upon the emergence of large-scale electrical vehicle manufacturing, the controlling units of vehicles are converted to electronic means. Mechanical control systems used for engine controlling, applying brakes and transmission are now being replaced by electronic control systems. Due to that, precise and smooth controlling can be achieved and could reduce the use of bulky mechanical components.

As an example Internal Combustion Engine, transmission system, differential system of a traditional vehicle could be replaced with two independent motors connected directly to rear wheels with a precise control mechanism. As presented in (Haiihosseinlu et al., 2014) the advantages of electronic control systems over conventional methods are listed below.

1. Avoided heavy, bulky mechanical arrangements. Energy efficiency of the vehicle is increased due to this.
2. Maximum turning angle of a normal vehicle is around 40 degrees. New model can support higher turning angles which gives more mobility options for the vehicle.
3. Due to the possibility of individual controlling of each wheel, it can provide better torque considering the traction surface for each wheel.

4. It is evident that adaptation of electronic controlling for a vehicle could provide above benefits.

2.1 The drive system of an EV

An Electric Vehicle's drive system performs the same functions as that of a vehicle powered by an internal combustion engine. The drive system is the part of the electric vehicle which transmits mechanical energy to the traction wheels causing the electric vehicle to move. Electric vehicles utilize an electric motor to rotate the wheels of the vehicles. There are several different drive system designs in use today. These include vehicles with a single large electric motor coupled to the rear wheels through a differential housing. Other designs utilize two smaller motors to power-up each wheel separately through independent drive shafts (Hashemnia & Asaei, 2008). As presented by (Draou, n.d.) and (Haiihosseinlu et al., 2014) this method is known as electronic differential system.Though the electronic differential system can be directly applied for electric vehicles, it is not widely found in available electric vehicles in the market (Madaras et al., 2013). Most of the EV employs mechanical differential connected to electric motor method as depicted in Fig. 1.

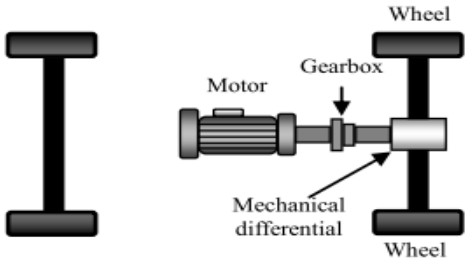

Figure 1: Arrangement of mechanical differential of a vehicle

3 DEVELOPMENT OF MATHEMATICAL MODEL FOR WHEEL SPEED RATIO CALCULATION

The relationship between steering angle, vehicle speed and speeds of rear wheels have to be derived by a mathematical model. The Ackerman Steering Principle (Yildrim et al., 2015)defines the geometry that is applied to all vehicles to enable the correct turning angle of the steering wheels to be generated when negotiating a corner or a curve. The intention of Ackermann geometry is to avoid the need for tyres to slip sideways when following the path around a curve. In order to ensure an ideal rolling of the wheels during cornering all wheels need to have their axles arranged as radii of a circle with a common centrepoint.

As the rear wheels are fixed, this centre point must be on a line extended from the rear axle. In order to intersect this rear wheel axis with the axes of the front wheels it requires the inside front wheel is turned, when steering, at a greater angle than the outside wheel. This is depicted in Fig. 2. Note that the angle of inner front wheel (β) is greater than the angle of outer front wheel (α).

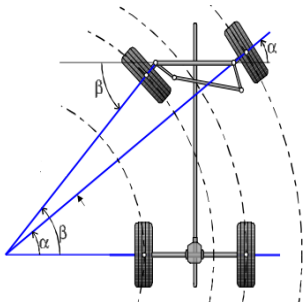

Figure 2: Geometrical arrangement of wheels in a turn (Vehicle is taking a left turn)

3.1 Relationship between inner and outer wheel speeds

Mathematical model will address the relationship of speeds of inner and outer wheels of the vehicle considering the turning angle of the vehicle. Fig. 3 depicts the parameters we consider upon construction of the model. The detailed geometry of a vehicle, presented by (Fu et al., 2012) for slide slip control is used here.

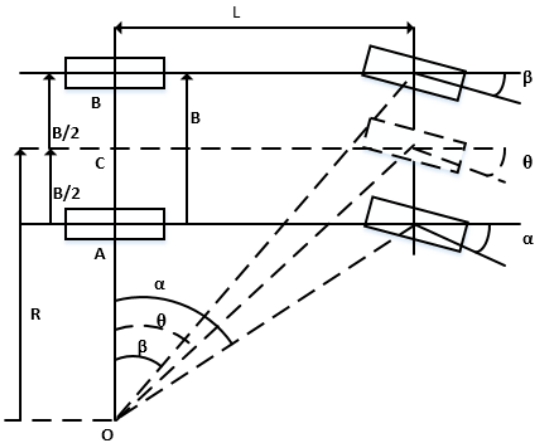

Figure3: Geometrical representation of wheels in a turn with parameters

R – Cornering radius B – Track width of the rear axel

L – Wheel base 0 – Centre of cornering

α – Angle displacement of front right wheel β – Angle displacement of front left wheel

θ - Angle of displacement of imaginary middle wheel also the steering angle of vehicle

The diagram shown in Fig. 3 illustrates a vehicle having four wheels. When the vehicle is steered by angle θ, the inner and outer wheels should be turned by α, β angles respectively. This is accommodated by the steering rack of the vehicle. It should be noted that the steering angle is changed by the driver and inner-outer wheel angles depend on that steering angle. Therefore θ is an independent variable and α, β are dependent variables.
When the vehicle is moving forward

$\theta = \alpha = \beta = 0^{o}$

When taking a turn it is

$\beta < \theta < \alpha$ for right turns or $\alpha < \theta < \beta$ for left turns.

3.2 Derivation of equations for wheel speeds

Step1

Referring to the diagram shown in Fig. 3, the radius of the curve can be expressed by the angles of the front wheels.

$$R = OC = \left(OA + \frac{B}{2}\right) = (OB - \frac{B}{2})$$

$$OA = L\ COT\ \alpha\ ,\ \ OB = L\ COT\ \beta$$

$$\therefore \mathbf{R = L\ COT\alpha + \frac{B}{2} = L\ COT\beta - \frac{B}{2} = L\ COT\ \theta}$$

It is clear that both inner and outer wheel angles have a relationship to steering angle. The steering angle can be represented by a single imaginary middle wheel angle. The control algorithm for rear wheel motor driven vehicles is developed based on this imaginary middle wheel concept. As presented by (Sharma & Pegu, 2015) this method can replace the initial four wheel model; hence reduce the complexity of calculations. This replacement model is illustrated in Fig. 4.

Step 2

It is possible to calculate the relationship between θ,α,β

$$\frac{B}{2} = R - L\ COT\alpha$$

$$R = L\ COT\beta - \frac{B}{2}$$

Substitute R and $\frac{B}{2}$

$$L\ COT\ \theta = L\ COT\beta - L\ COT\ \theta + L\ COT\alpha$$

$$COT\ \theta = \frac{(L\ COT\beta + L\ COT\alpha)}{2}$$

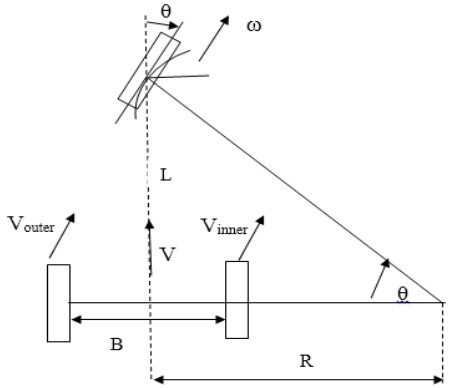

Figure4: Simplified geometric model with parameters

V – Vehicle linear speed ω – Vehicle angular speed
V_{inner} – Linear speed of inner wheel V_{outer} – Linear speed of outer wheel

Step 3 - The distance between center of rotation and vehicle's center line is given by

$$R = \frac{L}{\tan \theta} \tag{1}$$

Step 4 - The linear velocity equations of the left and right wheels can be derived based on the following equations. From the top view, the centers of both driven wheels of the vehicle are spinning with equal angular velocity about the point 0.

$$V = \omega R \tag{2}$$

Both wheels have the same angular velocity about the point 0, but different distances from the center of rotation. These different distances are creating the angles as discussed in section 3. Therefore when $\theta \neq 0$,

$$V_{inner} = \omega \left(R - \frac{B}{2}\right) \tag{3}$$

$$V_{outer} = \omega \left(R + \frac{B}{2}\right) \tag{4}$$

By substituting ω from (2) and R from (1)

$$V_{inner} = \frac{V}{R}\left(R - \frac{B}{2}\right) \quad , \quad V_{inner} = V\left[1 - \left(\frac{B \tan\theta}{2L}\right)\right] \tag{5}$$

$$V_{outer} = \frac{V}{R}\left(R + \frac{B}{2}\right) \quad , \quad V_{outer} = V\left[1 + \left(\frac{B \tan\theta}{2L}\right)\right] \tag{6}$$

If the wheel radius is R_d, the speed of each wheel in revolutions per minute (RPM) can be calculated as

$$\text{RPM inner} = V_{inner}\left|\frac{60}{(2\pi R_d)}\right| \tag{7}$$

$$\text{RPM outer} = V_{outer}\left|\frac{60}{(2\pi R_d)}\right| \tag{8}$$

4 FORMULATION OF THE CONTROL ALGORITHM FOR THE MATHEMATICAL MODEL

DC motor has almost linear relationship between speed and torque (Ramesh et al., 2011). For an electronic differential, two motor speeds are equal when the vehicle is running on a straight path and different when taking a turn. In a turn, inner wheel speed is less than outer wheel speed. Another point is that the two wheels may not always travel in identical surfaces of the road. If one wheel moves on an inclined surface on the road, the particular motor has higher load than the wheel moves on a flat surface. Therefore the motor attached to this wheel, has to generate a higher torque than latter one. A speed control algorithm is required to overcome this issue.

4.1 DC motor speed and torque controlling by PWM method

It can be shown that the speed of a DC motor can be controlled by the duty cycle of the pulse width modulated (PWM) signal given to motor (Haiihosseinlu et al., 2014). PWM signals with higher duty cycles will have higher conduction time hence provide higher speeds. If the load on the motor is high, for the same PWM signal, the motor tends to reduce the speed. In this situation, the duty cycle of the PWM signal has to be increased in order to retain the required speed (Haiihosseinlu et al., 2014). Fig. 5 illustrates the DC motor speed torque characteristic curves for three different PWM signals shown as PWM1, PWM2 and PWM3. In this illustration, PWM 3 has the highest duty cycle which is 100%. It is possible to vary the duty cycle under PWM 3 curve region.

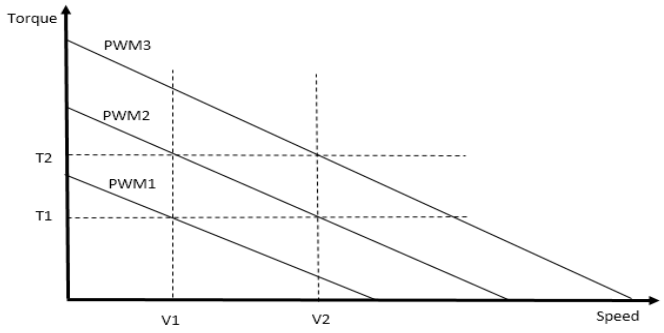

Figure 5: DC motor torque speed characteristics in different PWM signals

As an example, if T2 is the torque for rough road surface and T1 for smooth road surface, the speed V1 can be maintained by changing the PWM duty ratio. By changing the duty cycle; it is possible to move the characteristic curve parallel to each other as PWM 1, PWM 2 and PWM 3 below 100% duty cycle. By considering the above graph it is possible to deduce the required PWM signal for each motor considering the drive pattern, required velocity and the torque. Following table denotes the possible combinations for torque and velocity and the required PWM signal for each motor. Table 1 shows different combinations of PWM signals for inner and outer wheels which will provide the necessary speeds at different requirements of torques for each wheel. It represents two speeds named V1 and V2 and two torques named T1 and T2 which are interpreted as requirements for two different loads on wheels. In the case where the vehicle run on a straight path and the surface is same for both wheels, the required torque will be same. Therefore same PWM will be applied to the motors. If one of the wheels runs on a

different surface than the other one, the speed requirement is same for both wheels but the torque is different. Therefore, to compensate the torque it is required to change the PWM of one motor. It will maintain the desired speed by applying different torques on two wheels. The Table 1 shows examples for twelve different circumstances.

Table 1: PWM signal for different circumstances

Drive path	Inner wheel Load	Outer wheel Load	Inner wheel speed	Outer wheel speed	Inner wheel torque	Outer wheel torque	Inner motor PWM	Outer motor PWM
Strait run	Low	Low	V1	V1	T1	T1	PWM 1	PWM 1
Strait run	Low	High	V1	V1	T1	T2	PWM 1	PWM 2
Strait run	High	Low	V1	V1	T2	T1	PWM 2	PWM 1
Strait run	High	High	V1	V1	T2	T2	PWM 2	PWM 2
Turning	Low	Low	V1	V2	T1	T1	PWM 1	PWM 2
Turning	Low	High	V1	V2	T1	T2	PWM 1	PWM 3
Turning	High	Low	V1	V2	T2	T1	PWM 2	PWM 2
Turning	High	High	V1	V2	T2	T2	PWM 2	PWM 3
Strait run	Low	Low	V2	V2	T1	T1	PWM 2	PWM 2
Strait run	Low	High	V2	V2	T1	T2	PWM 2	PWM 3
Strait run	High	Low	V2	V2	T2	T1	PWM 3	PWM 2
Strait run	High	High	V2	V2	T2	T2	PWM 3	PWM 3

From table1, it is evident that different torque and speed requirements can be achieved by providing the correct PWM to the motor. In order to define the correct wheel speed ratio the mathematical model derived in section 3.2 is used. It is then used to generate the correct PWM by an algorithm. Fig. 6 shows the flow chart of the control algorithm.

4.2 PID control method

It is observed that the ratio between outer wheel speed and inner wheel speed depends on steering angle (θ) and does not depend on speed. This can be proved from the equations (5) and (6) since the parameters B and L are constants and only variable is (θ). For smooth functioning of differential, the speed ratio has to be maintained with minimum error.A proportional-integral-derivative (PID) controller can calculate an error value as the difference between a measured process variable and a desired set point. The controller attempts to minimize the error by adjusting the process through a manipulated variable. In the prototype the error is the difference between set speed and the measured speed of a wheel. In order to minimize the error it varies the duty ratioof the PWM to retain the desired speed of the motors. Arduino® has PID library which could be directly used to get the calculated outputs efficiently.

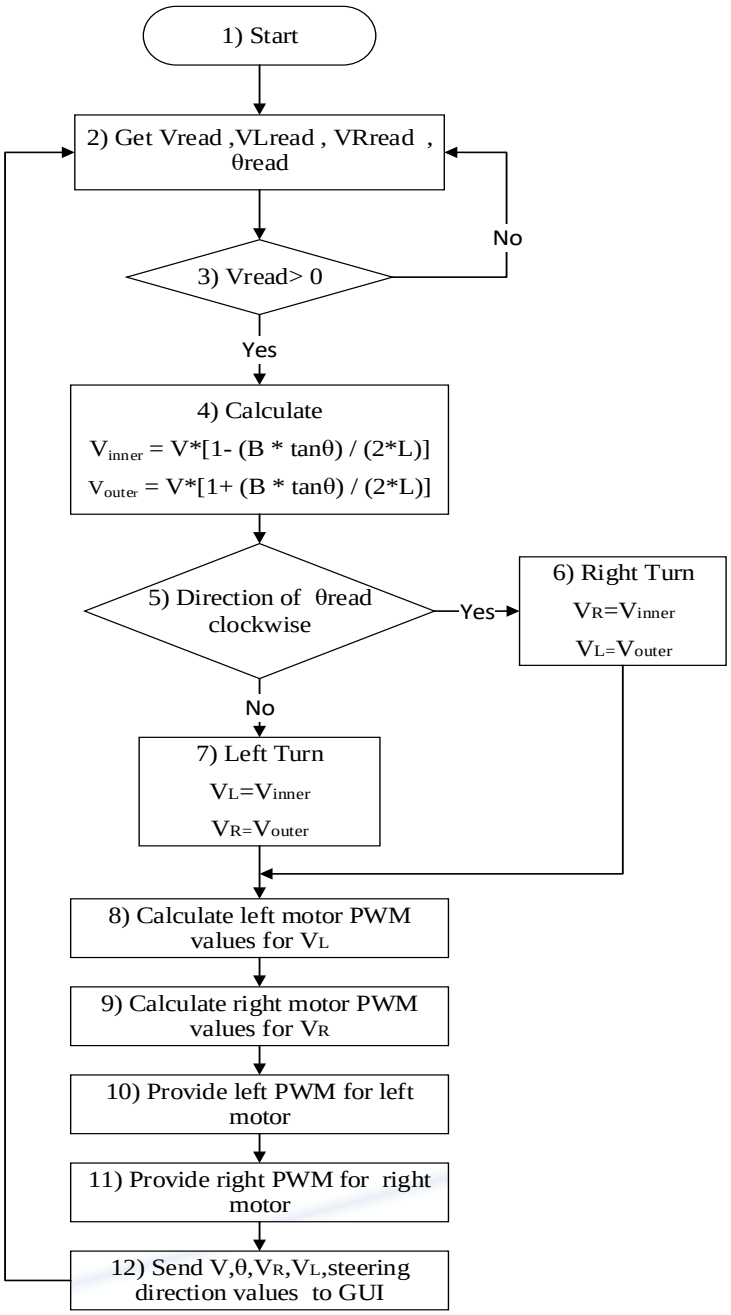

Figure 6: Flow chart of the control algorithm

4.3 Testing of the algorithm using the prototype

The algorithm has been tested on a prototype model of a vehicle. Design of the prototype was based on following facts.

1. Type of the motor – There are several motor types found in electric vehicles. Induction motor is used by most of the vehicle manufacturers considering its characteristics. For the construction of prototype, controllability of the motor is the first priority in selection of a motor. DC motors has the highest controllability and cost of controller is comparatively low. Therefore DC motors have been used for constructions which were controlled by PWM method.

2. Motor drive – The drive for the prime mover of the vehicle. The L298 drive was used as motor drive.

3. Energy source – The battery should be capable to provide power to the prototype.

4. Microcontroller – Prototype works according to the control algorithm. Therefore a microcontroller was required to run the algorithm. This algorithm has mathematical calculations and outputs should be precise. Since the model should be capable of providing results while running the vehicle the microcontroller should have sufficient processing speed.

4.3.1 Control system of the prototype

As shown in Fig. 7 the control system of the prototype consists of speed and steering angle as inputs.

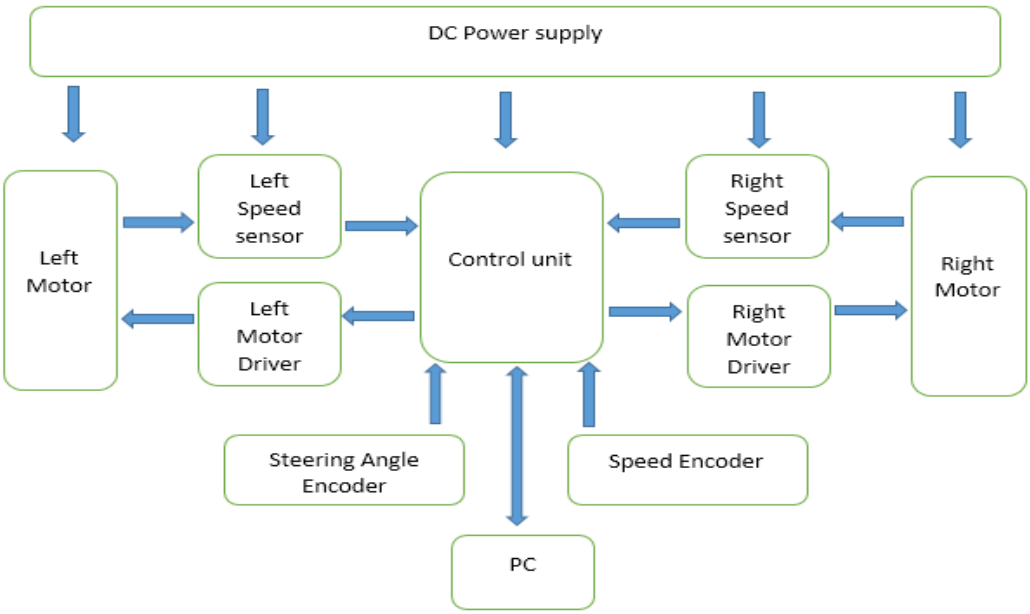

Figure 7: Block diagram of the control of prototype

Two volume control type potentiometers have been used to give the inputs to controller. Those are connected to A0 and A1 analog input pins of Arduino board. The Arduino microcontroller reads 0 – 5 V analog input range with a resolution of 8 bit binary numbers. This means it reads the 0 – 5 V analog range in 28 = 1024 voltage steps. By program code, the read value is mapped to desired range of speed and steering angle parameters. The input denotes the input limits and read values. Table 2 compares the input ranges of the Arduino microcontroller and the relevant input variable.

Table 2: Input variables and relevant ranges of the Arduino microcontroller

Input	Voltage range	Microcontroller pin	Microcontroller reading range
Speed	0 V to 5 V	A0	0 RPM to 350 RPM
Steering angle	0 V to 5 V	A1	40 Degrees to – 40 degrees

As described in PID method the control system requires a feedback from the wheel speed. Therefore a sensor is attached to the drive motors to measure the wheel speed. The sensor is a rotary encoder which has 20 holes on the rotating disc. When the encoder wheel rotates together with the motor drive shaft, it generates a digital pulse train cycled at the rate of wheel speed. For a complete rotation, the encoder generates 20 pulses. Encoder outputs are connected to the interrupt handling pins of Arduino. When the pin receives a rising edge of a pulse, it calls for interrupt handling subroutine of the main program which calculates the speed of the wheel.

4.3.2 Driving of motors

The duty cycle for PWM can be varied in steps of 1 in the range of 0 to 255 in Arduino® PWM output. PWM value for required speed is calculated by PID subroutine. Arduino has a PID library which calculates the required PWM output for the motor drive. The inputs for the PID function are the set speed, measured speed and the P, I, D constants. Values for the constants are determined by manual tuning method. Here the values are changed until the desired performance level is achieved.

4.3.3 Design considerations of PWM generation

Maximum RPM of the selected motors are around 520 rpm. If the motor rotates at this speed, it generates much heat and noise. This reduces the lifetime of the motor. Therefore maximum rpm is limited to 350.

The tested Motors do not rotate for a PWM value fewer than 35. Because the voltage applied at that level is insufficient to overcome the internal losses and start motor rotation. Minimum rpm for the motors has been decided as 40. Speeds from 40 rpm to above could be directly achieved by PWM. Speeds below 40 rpm cannot be achieved by PWM controlling. For a real model these lower speeds could be achieved by applying wheel brakes.

5 REAL TIME TESTING AND RUN TIME MEASUREMENTS

The prototype control system has been tested for two control scenarios. Test 1 was the straight run of the vehicle with varying speeds. The steering input is set to zero for this test run. Test2 was the changing steering angles for constant speed input.

5.1 Real time testing and data acquisition

Data acquisition has been done by using MegaunoLink® (Marketing, 2015) software.

Measurements of each test run are as follows.

i. Left Wheel Speed measured
ii. Right Wheel Speed measured
iii. Speed Input
iv. Steering Input

From the measurements, following information has been calculated.

PWM for inner and outer wheel from equation (7) and (8)

Desired speed ratio = (Inner wheel set speed / Outer wheel set speed)

Actual speed ratio = (Inner wheel measured speed / Outer wheel set speed)

Ratio error = (Desired speed ratio – Actual speed ratio)

Inner or outer wheel speed error = (Set speed – actual speed) / set speed

5.2 Analysis of results

Test1 – Steering input is fixed at zero. Seven different speeds have been given to the input throughout the run. Test has been run for forty seconds. Eighty data points at equal time intervals have been measured using MegaunoLink® data acquisition and recorded on computer. The requirement of this scenario is to maintain the speeds of inner and outer wheels speed ratio at unity when vehicle speed change occurs. The graph in Fig. 8 shows the actual speed change of each wheel along with the set speed variation. It is evident that the controller is taking a time to fix the wheel speed to the desired value. The prototype has been tested with minimum load on vehicle. Therefore the fluctuations of speed measurements have been shown. More loading on wheels will damp the sudden variations in a real model. The PID controller has been tuned to get the step response to an acceptable smooth level.

Test2 – Vehicle speed is fixed and different steering angles have been given to the input throughout the run. Test has been run for fifty five seconds. One hundred and ten data points have been acquired using the same methodology as test1. The requirement of this scenario is to set the correct speed ratio immediately after changing the steering angle. Fig. 9 shows the actual wheel speed variation for steering input changes with constant vehicle speed. From the results it is evident that the controller follows the desired speed of each wheel and correctly changes the speed at desired point. According to the PID controller values it takes a time to stabilize the speed of wheel.

5.2.1 Average error calculation for the test run

From the results, the error ratio for the wheel speed can be calculated as

Speed error = (set speed – actual speed) / set speed

The average speed error has been calculated for the period of entire test run of test1 and test2 separately. The results show that for the test1 the average speed error is 0.06. For test2 it is 0.07 for left wheel speed and 0.08 for right wheel speed. According to the results it is evident that the controller is capable of setting the desired speed more accurately for speed changes than changes in steering input.

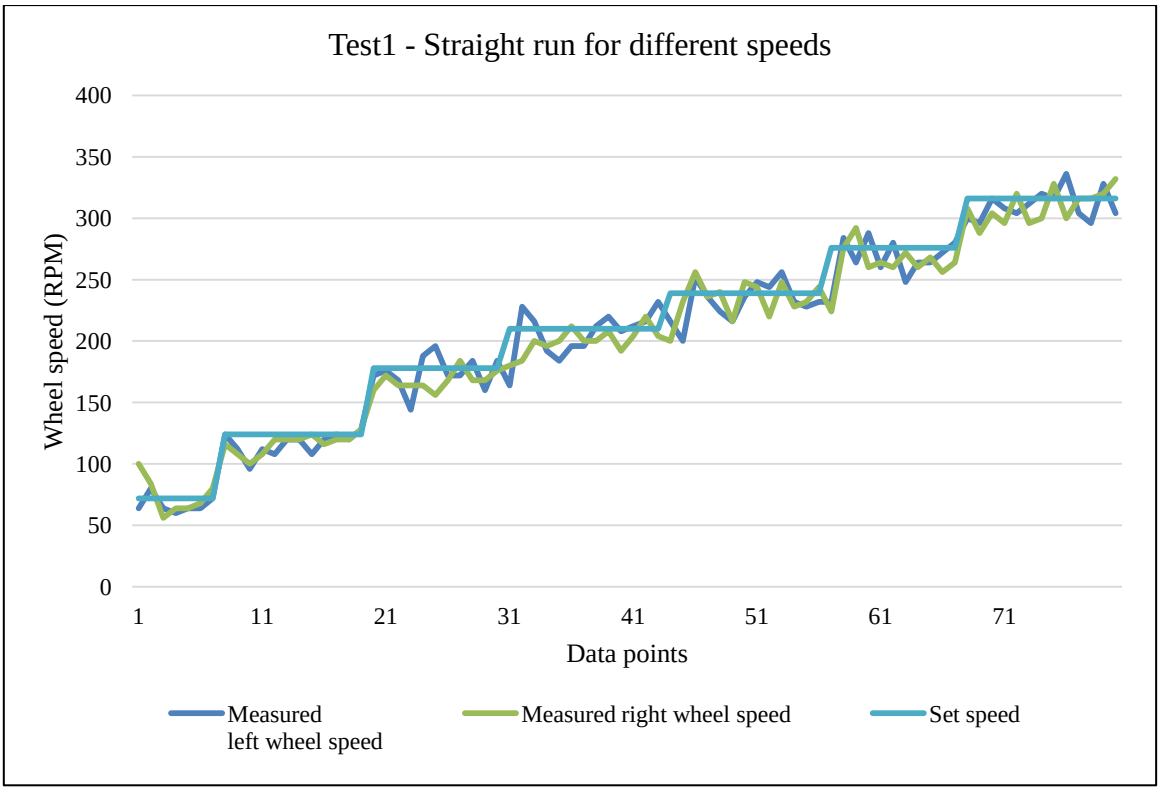

Figure 8: Actual wheel speed variation according to set speed changes

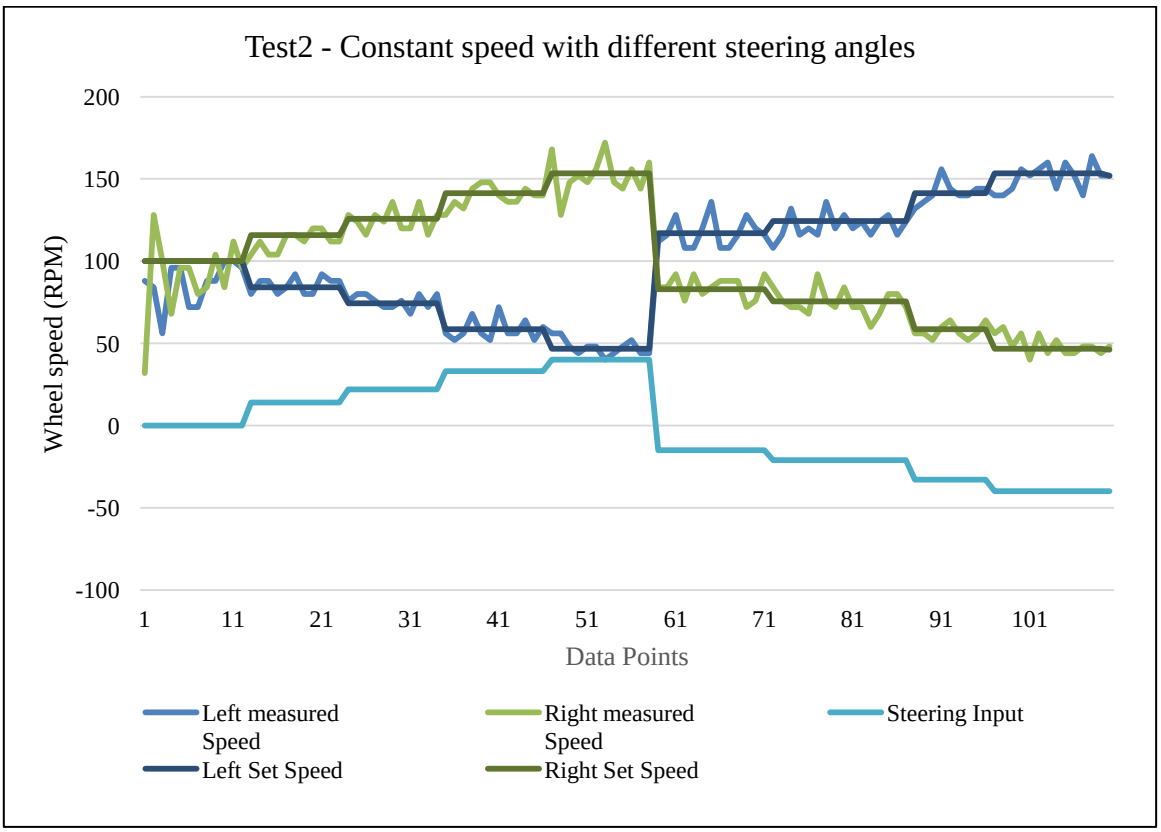

Figure 9: Actual wheel speed variation according to steering input changes

6 CONCLUSION

The mathematical model designed for the electronic differential concept has been tested with a prototype. Test results have confirmed the correctness of the control algorithm hence prove the mathematical model. There are differences between the calculated values and the measured values. A real implementation model can test how much tolerance is acceptable without disturbing traction. Following points have been identified as possible reasons for the error between expected and test results.

The two motors which are connected to left and right wheels have to be almost identical in its physical parameters. Otherwise it is not possible to have same measurements as Rise time, Settling time for the two motors. The motors which are used for the prototype are manufactured not exclusively for this purpose. For a real application, DC traction motors has to be uniquely manufactured.

The Atmega® microcontroller in Arduino® board does not support multi-threading operation. Therefore all the functions (read inputs, measure speed, calculate PID outputs) has to be done in same control loop in the program code. The speed measurement subroutine has 750 milliseconds delay for one wheel speed measurement, altogether the control loop delayed for 1.5 seconds interval during speed measurements. This is affecting for the performance of the system. This could be overcome by using a multithreading support microcontroller and measuring the wheel speeds in different threads. This method is useful for a practical Electronic Differential design.

It is clear that the mathematical model is proven for giving correct inner and outer wheel speed ratio when steering a vehicle. By using this model, the conventional differential can be replaced with electronic counterpart hence achieve more benefits for the vehicle manufacturing industry. The differential lock method which is used in heavy vehicles can also be achieved with this electronic differential method. It is required when one of the two rear wheels is on a slipping surface while the other is on rough surface. Then the wheel on the sipping surface tends to run at a higher speed unless the differential is mechanically locked. In this electronic differential method this kind of wheel slip will not be occurred. Because it gets the wheel speed as a feedback and the control system set the PWM to maintain that desired speed. Therefore this kind of wheel slipping will not be occurred with electronic differential method.

Even though the current approach was to design a differential for rear wheel motor driven vehicle, it is possible to improve this technology to drive front wheel and all-wheel drive vehicles as well.

REFERENCES

1. Baily, R., 2014. *College of Engineering and Computer Science*. [Online] Available at: http://www.utc.edu/college-engineering-computer-science/research centers/cete/electric.php[Accessed 2015].

2. Draou, A., n.d. Electronic differential speed control for two in-wheels motors drive vehicle. In *Fourth International Conference on Power Engineering, Energy and Electrical Drives (POWERENG), 2013*. Istanbul IEEE.

3. Fu, C., Hoseinnezhad, R., Bab-Hadiashar, A. & Watkins, S., 2012. Electronic differential design for vehicle side-slip control. In *International Conference on Control, Automation and Information Sciences (ICCAIS), 2012*. Ho Chi Minh City, 2012. IEEE.

4. Haiihosseinlu, A., Filizadeh, S. & Dirks, E., 2014. Electronic differential design for a vehicle with four independently controlled in-wheel motors. In *Electric Vehicle Conference (IEVC), 2014*. Florence, 2014. IEEE International.

5. Hashemnia, N. & Asaei, B., 2008. Comparative Study on Different Electric Motors in Electric Vechicles. In *18th International Conference on Electrical Machines*. Vilamoura, 2008. ICEM 2008.

6. Home, A., n.d. *Arduino Board - UNo*. [Online] Available at: http://www.arduino.cc/en/Main/ArduinoBoardUno [Accessed 2015].

7. Madaras, J., Bugar, M. & Danko, J., 2013. Driving Dynamics of an Electric Vehicle with an Electronic Differential. Bratislava, 2013. Faculty of Mechanical Engineering STU.

8. Marketing, F.D.M.&., 2015. *Megunolink*. [Online] Available at: http://www.megunolink.com/ [Accessed 2015].

9. Ramesh, M.V., Rao, G.S., Kamakshaiah, S. & Jawaharlal, B., 2011. Speed torque characteristics of brushless DC motor in either direction on load using ARM controller. In *Innovative Smart Grid Technologies - India (ISGT India), 2011*. Kollam, Kerala, 25 March 2011. IEEE PES.

10. Sharma, S. & Pegu, R., 2015. Electronic differential for electric vehicle with single wheel reference. In *1st Conference on Power, Dielectric and Energy Management at NERIST (ICPDEN)*. Itanagar, 2015. IEEE.

11. Tejas Krishna Kshatriya, A.V.S., 2013. *Motor Differential*. [Online] Available at: http://www.google.com/patents/WO2013108265A3?cl=en

12. Yildrim, M., Oksuztepe, E. & Kurum, H., 2015. Design of Electronic Differential System for an Electric Vehicle with in-wheel motor. In *2016 IEEE Power and Energy Conference at Illinois (PECI)*. Urbana, IL, 2015. IEEE.

Study the Physical Property Variations of Core Spun Cotton-Spandex Single Jersey Fabrics under Relaxation

C. N Herath

Department of Textile and Apparel Technology, Faculty of Engineering Technology, The Open University of Sri Lanka, Nawala, Nugeoda, Sri Lanka.

Corresponding Author: email: chera@ou.ac.lk, Tele: +94112881065

Abstract – *In this research, variations of structural spacing, stitch density, fabric thickness, areal density, fabric stiffness, flexural rigidity, air permeability, and bursting strength properties of cotton/spandex and cotton single jersey structures have investigated. These fabrics were knitted in high, medium and low stitch lengths and subjected to dry-, wet-, full- relaxation and washing treatments. Cotton/spandex structures have given higher stitch densities and lower structural spacing, higher areal densities and higher fabric thickness values than cotton structures. These physical properties increased with progression of treatments and structural spacing have decreased in further relaxation of stitches. They have shown good positive correlation with fabric tightness factor (stitch length^{-1}), but structural spacing had the negative correlation. Higher bending lengths and flexural rigidities have also given by cotton/spandex than cotton structures. Those properties are higher in course direction than in wale direction and positively correlate with stitch length^{-1}. Air permeability has given positive correlation with stitch length and also given lower air permeability with cotton/spandex structures. Bursting strength has shown positive correlation with stitch length^{-1} and higher values at higher treatment levels. Cotton/spandex structures have given higher bursting strengths compared to cotton. All the considered physical properties are significantly influenced by the machine set stitch lengths, the relaxation level and material type.*

Key words: *Cotton/spandex, single jersey fabrics, physical property, air permeability, bursting strength*

Nomenclature

CO-SP: Cotton/spandex	CO: 100% Cotton	TF: Tightness factor
H-TF: High tightness factor	M-TF: Medium tightness factor	L-TF: Low tightness actor
WPC^{-1}:Wales/cm	CPC^{-1}:Courses/cm	

1. INTRODUCTION

It is well known fact that structural changes take a place in knitted structures during relaxation treatments and laundering treatments (Sharma *et.al.* 1985), (Marmarali, 2003), (Herath and Kang, 2008). This may cause for the variations of physical properties of these fabric structures. It depends mainly on the fiber type, structure type, structural tightness factor, knitting conditions, relaxation and laundering treatments etc. This variations of physical properties effect on the performance, functional qualities, durability, aesthetic qualities etc. of these knitted fabrics (Hepworth 1982), (Herath and Kang, 2008).

Previous researches were carried out to investigate the physical property variations of several various knitted structures such as single jersey, rib, interlocks made from cotton, acrylic, polyester, polyamide and some of their combinations under the applications of various relaxation techniques (Sharma *et.al.* 1985), (Herath and Kang, 2008) (Mayruz and Ogulata, 2010). Results indicated that thickness, areal density, flexural rigidity, shear rigidity, stiffness, bursting strength of tested structures have significantly effected by stitch type, structural tightness factor, yarn composition, relaxation treatments etc.

(Sharma *et.al.* 1985), (Ertugrul and Ucar 2000), (Marmarali, 2003), (Herath and Kang, 2008). Thus, one research on the certain physical property variations such as thickness, areal density, air permeability of cotton-spandex made with full and half plated single jersey fabrics has reported that these properties significantly changed with the relaxation treatments (Marmarali, 2003).

In this experiment, variations of physical properties such as structural parameter variations, air permeability, fabric thickness, fabric stiffness and bursting strength of core spun cotton-spandex single jersey fabrics were investigated under various relaxation and laundering treatments. Thus, results are compared with those for similar fabrics knitted from 100% cotton yarns.

2. EXPERIMENTAL

Materials

Single jersey fabrics made from core spun (93 % of cotton and 7 % of spandex) cotton/spandex and cotton were knitted in a circular knitting machine in high, medium and low tightness factors. Ring spun unmerzerised cotton (30 Ne) and 40decitex "Creora" spandex filaments from Hyosung company, Korea, were used for spinning of cotton/spandex yarns. Table 1 gives yarn characteristics and knitting details are given with Table 2. In order to maintain sufficient tension, 6 cN was selected as an in-put tension for CO-SP yarns to knitting zone, based on the series of pre-experiments.

Selected machine set stitch length for CO-SP and CO single jersey fabrics are given in Table 3. These stitch lengths have been set in the machine using the setting of stitch cams, and stitch lengths were measured according to the standard procedure. Based on that TFs were classified as H-TF, M-TF and L-TF. In this table, machine off stitch lengths, which were calculated under 95% significant level, are given in parenthesis. It is clearly shown that, even though the machine set stitch lengths are same for both CO and CO-SP structures, the machine off stitch lengths are different, which is due to the "robin back effect" and the differences are given in square brackets in Table 3 as percentages. According to that, higher reductions show with CO-SP structures. Reason would be the higher resiliency property of CO-SP yarns. Thus, robin back effect decreased by increasing the tightness factor in CO-SP structures. But, CO fabrics show an opposite behavior.

Table 1: Yarn characteristics used for knitting

Single jersey Material	Nominal count [Ne]	Measured count [tex]	Tensile strength [gf]	Extension at break [%]	Yarn twist [tpi]
CO-SP	30	20.40	305.0	8.94	24.41
CO	30	20.14	359.8	5.04	19.70

Table 2: Knitting details

Single jersey material	Machine diameter [inches]	Gauge	Machine RPM	No. of positive feeders	No. of needles
CO-SP and CO	30	28	22	72	2640

Table 3: Machine set stitch lengths in mm

Material	L-TF	M-TF	H-TF
CO-SP	2.90(2.68±0.020) [7.59%]	2.70(2.55±0.012) [5.55%]	2.50(2.40±0.010) [4%]
CO	2.90(2.84±0.021) [2.07%]	2.70(2.62±0.032) [2.96%]	2.50(2.42±0.041) [3.2%]

Method

Sample preparation: Sample size of 30x30 cm^2 were cut from cotton and cotton/spandex single jersey fabrics. Six samples were cut from knitted structures from each tightness factor. Samples were first subjected to dry- and wet- relaxation and then subjected to full relaxation followed by laundering treatments as given below. Relaxation treatments were done according to ASTM D 1284-76 and washing treatments were followed ISO 6330 standards.

Dry Relaxation: Samples were placed in a conditioning cabinet for 48 hours under standard temperature of 21±1^{0}C and relative humidity (RH) of 65%±2)

Wet Relaxation: Dry relaxed samples were wetted in a water bath containing 0.05g/l of standard wetting agent, maintaining the temperature at about 38^{o}C for 24 hours with minimum agitation. Samples were hydro-extracted and put in a conditioning cabinet for 48 hours under standard conditions (21^{o}C±1 at RH of 65%±2).

Full Relaxation: Wet relaxed samples were washed thoroughly, briefly hydro extracted for 1 minute and tumbler dried for 60 min. around 70 ^{o}C. Samples were then laid on a flat surface in a conditioning cabinet for 48 hours under standard conditions.

Washing treatments*:* Fully relaxed samples were laundered 1st to the 5th cycle (W1 to W5)in a standard front loading machine under normal agitation. Washing temperature was set at 40^{0}C and rinsed with cold water and 0.1g/*l* standard wetting agent was used and mass of the total load was maintained as 3kg. After tumble drying for 60 minutes, samples were brought to the standard conditions.

According to the literature survey, structural changes occur during relaxation and washing treatments in the weft knitted fabric structures, which may cause for the variations of the physical properties of the fabrics affecting on the end uses. Therefore, structural spacing variations and stitch density variations of single jersey structures were measured according to the standard practice.

To measure the areal density (g/ m^2), sample size of 30×30cm^2 (from the middle area of the relaxed fabric type) were cut after each treatment stage. Then, 10 specimens per each tightness factor for each treatment stage were prepared and weight measurements were taken from standard electronic balance within 0.1% accuracy. This experiment was done according to the ASTMD 3776-96.

In measuring fabric thickness, standard digital thickness gauge meter with 40mm diameter of base plate, 14mm diameter of pressure foot and pressure of 3.42 k Pa (35g f/ cm^2) were used. Measurements were taken at 5 random places per specimen. That means, there were 30 data collected per tightness factor of each single jersey fabric type. This test was done according to the ASTMD 1776-96 (2002). Air permeability test was carried out using standard air permeability tester with test area of 38cm^2 and imposed air pressure of

125 Pa. There were five areas in a fabric specimen were subjected to this test and altogether 30 data were collected per tightness factor per single jersey structure. This experiment was carried out according to the ASTM D 737-96

In order to measure the bursting strength of single jersey weft knitted structures, Mullen type hydraulic standard bursting strength tester was used according to the ASTM D 3786 standard. Applied hydraulic pressure was 20 kg/m^2 and diaphragm diameter was 50cm^2 with 2mm thickness.

In measuring the fabric stiffness, ASTM D 1388-96 standard was used. For CO single jersey fabric samples, only the heart loop method was suitable, due to its curling of cut edges of the specimens. However, cantilever method could be used for CO-SP single jersey fabrics due to its higher stitch densities and higher fabric tightness factors.

3. RESULTS AND DISCUSSION

Structural spacing and stitch density variations

Figure 1 (a) and (b) shows the WPC^{-1} and CPC^{-1} variations of CO-SP and CO single jersey structures under relaxation and washing treatments.

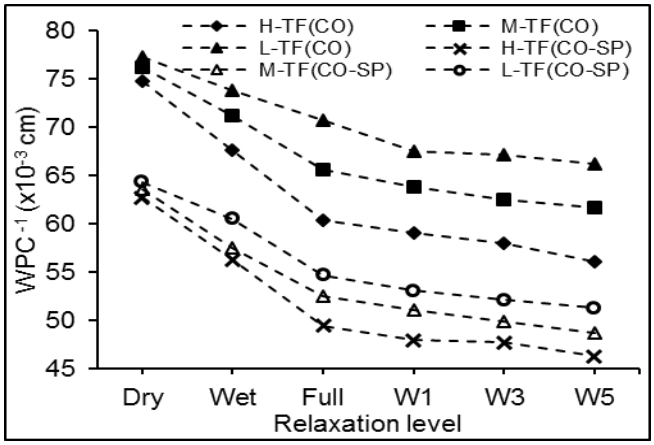

Knitted structure	Fabric TF	Spacing reduction % from dry relax-W5
CO	H-TF	24.96
	M-TF	19.16
	L-TF	14.37
CO-SP	H-TF	26.16
	M-TF	23.54
	L-TF	20.30

(a)WPC^{-1} variations

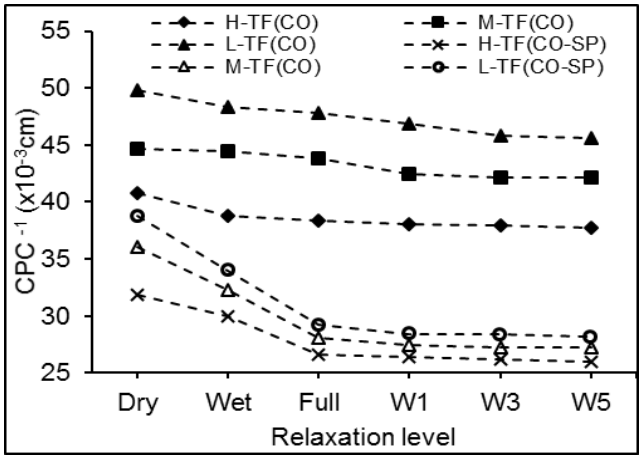

Knitted structure	Fabric TF	Spacing reduction % from dry relax-W5
CO	H-TF	24.96
	M-TF	19.16
	L-TF	14.37
CO-SP	H-TF	26.16
	M-TF	23.54
	L-TF	20.30

(b)CPC^{-1} variations

Figure 1: Structural spacing variations of CO and CO-SP single jersey fabrics

Figures show the higher wale spacing than course spacing in both the strictures and the structural spacing have significantly reduced with progressing the treatments as given in the tables with Figure1. Thus, steeper spacing reductions can be observed from dry relaxation to full relaxation in both CO-SP and CO structures compared to rest of the treatment. Thus, CO single jersey structures shows higher structural spacing than that of CO-SP single jersey structures. However, Figure 1 demonstrates very clearly that structural spacing positively correlates to the stitch length and reduction of spacing during treatments show a negative correlation to stitch length.

Figure 2 shows the stitch density variations of CO-SP and CO single jersey structures during the treatments. It shows that stitch densities increased with the progression of treatments as given in the table in Figure 2, because, plain stitches in the single jersey structures are more relaxed with the treatments specially contacting and agitation with water and also under tumbler drying, which results to change the stitch configuration during these relaxation treatments. Further, according to the table in Figure 2, stitch density increasing %s are positively correlates with the stitch density $^{-1}$ for CO structures and negatively correlates with the stitch density $^{-1}$for CO-SP single jersey structures.

Hence, CO-SP single jersey structures gave very high stitch densities than CO, even though both single jersey structures have knitted with same machine set stitch lengths. Reasons would be the lower machine off stitch lengths reported (as given in Table 3) with CO-SP due to their excellent stretch and recovering properties and robin back effect in knitting. Thus, Figure 2 shows that stich density variations negatively correlates to machine set stitch lengths. Steeper increases of stitch densities have given during dry relaxation to full relaxation of the samples. Stitch density variations shown in Figure 2 are caused by the structural spacing changes illustrated in Figure 1.

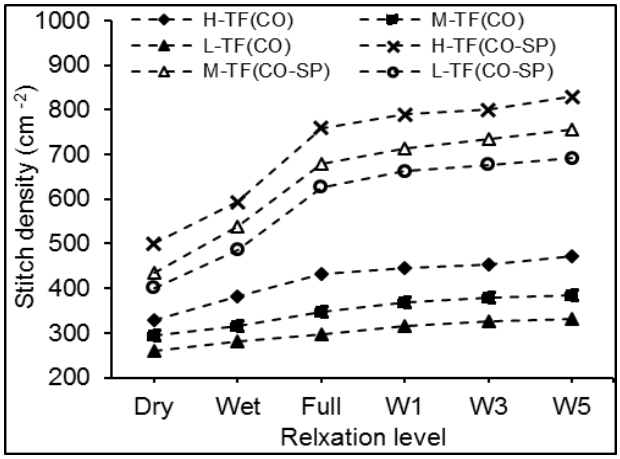

Knitted structure	Fabric TF	Stitch density increasing % from dry relax-W5
CO	H-TF	43.63
	M-TF	31.10
	L-TF	27.43
CO-SP	H-TF	65.70
	M-TF	73.33
	L-TF	72.49

Figure 2: Stitch density variations of CO and CO-SP single jersey fabrics

Fabric thickness variations

Figure 3 shows the fabric thickness variations of CO-SP and CO single jersey fabrics. It is very clear that CO-SP structures achieved significantly higher values than CO structures, even though both of these structures had the same machine set stitch lengths as given in the Table 3. Hence, according to the table given with Figure 3, it is very clearly showing that thickness of the single jersey fabrics increased with the progression of treatments and it positively correlates with stitchlength^{-1} or fabric TF in all the experimented cases of CO-SP and CO single jersey fabrics. However, CO-SP single jersey structures demonstrated

very significant deviations of fabric thickness variations with their fabric TFs than CO single jersey fabrics. Reasons for these variations would be that they get the higher stitch densities due to higher resiliency property of CO-SP yarns and it results more bending the stitches into third dimension due to the more relaxation of stitches. Thus, due to higher stitch densities, structural jamming of single jersey structures may also give support to increase the fabric thickness values of CO-SP structures compared to CO structures.

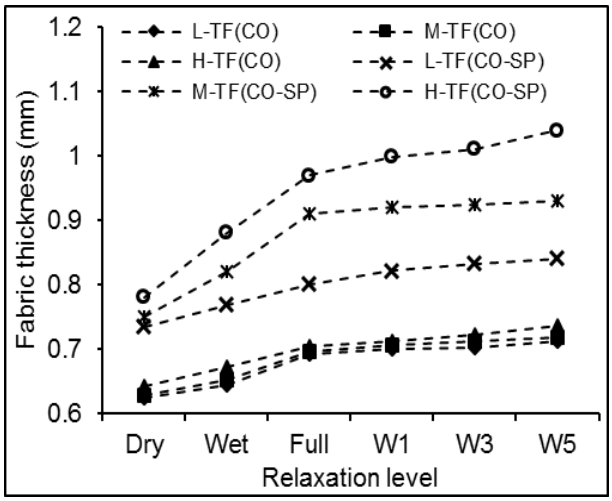

Knitted structure	Fabric TF	Fabric thickness increasing % from dry relax-W5
CO	H-TF	14.66
	M-TF	14.33
	L-TF	14.13
CO-SP	H-TF	33.21
	M-TF	24.00
	L-TF	14.44

Figure 3: Fabric thickness variations of CO and CO-SP single jersey fabrics

Fabric areal density variations

Fabric areal density is expressed as the weight in grams per unit area of a fabric. In industry, this is very frequently used to determine the quality of a fabric. Figure 4 shows the areal density variations of CO-SP and CO single jersey fabrics.

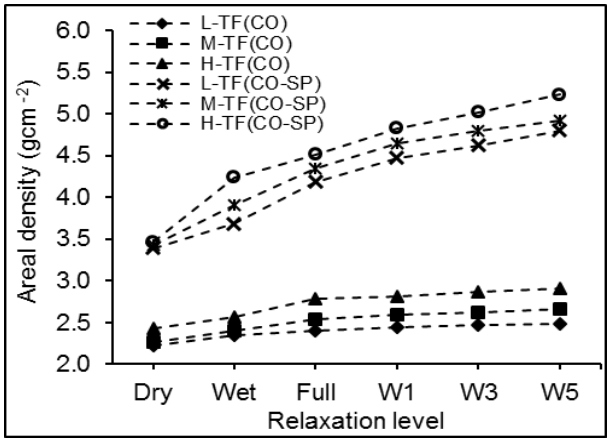

Knitted structure	Fabric TF	Area density increasing % from dry relax-W5
CO	H-TF	19.88
	M-TF	17.33
	L-TF	11.56
CO-SP	H-TF	51.17
	M-TF	43.51
	L-TF	41.53

Figure 4: Areal density (gm^{-2}) variations of CO and CO-SP single jersey fabrics

According to the Figure 4, areal density positively correlates with the fabric TF or stitch $length^{-1}$. Therefore, H-TF structures of CO-SP and CO single jersey fabrics gave significantly higher areal density values. However, CO-SP structures have given significantly higher areal densities than CO structures, even though both of these structures consisted of the same machine set stitch lengths in manufacturing. Thus, according to the table given with Figure 4, progression of treatments gives areal density

increases in both CO-SP and CO single jersey structures. Main reason for the increasing areal densities of CO and CO-SP single jersey fabrics is due to the changing of stitch densities with respect to the CO and CO-SP fabrics subjected to the treatments, as shown in Figure 2.

Stiffness property variations

Stiffness is one of the main properties of textile fabrics in relation to the drapability and several other functional properties such as handle, comfort properties etc. In this research, stiffness has been expressed in terms of bending length and flexural rigidity.

Figure 5 and 6 shows the variations of bending length of CO-SP and CO single jersey fabrics in wale (indicated in figure by *W)* and course (indicated in figure by *C*) directions. It is shown that CO-SP single jersey structures have given higher bending lengths than CO structures in both wale and course directions. Thus, in both fabric types, higher stiffness (due to higher bending lengths) are given in course direction than that of wale direction. Reason could be the higher course cm^{-1} (measured as 20.07 -24.55 and 25.8-31.4 courses/cm in CO & CO-SP respectively at dry relax and 21.9 -26.49 and 35.47-38.42 courses/cm in CO and CO-SP respectively after W-5) than wale cm^{-1} (measured as 12.73 - 13.38 and 15.55-15.95 wales/cm in CO & CO-SP respectively at dry relax and 15.1 -17.83 and 19.51-21.6 wales/cm in CO and CO-SP respectively after W-5).

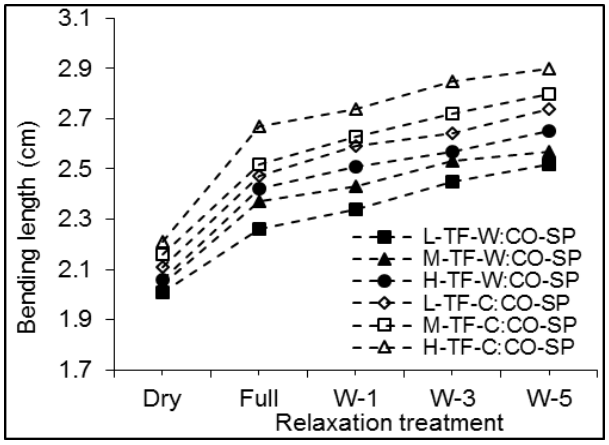

Knitted structure	Fabric TF	Bending length increasing % from dry relax-W5
CO	H-TF	20.00
	M-TF	19.43
	L-TF	21.18
CO-SP	H-TF	20.92
	M-TF	21.51
	L-TF	22.09

Figure 5: Bending lengths of CO-SP fabrics in wale and course directions

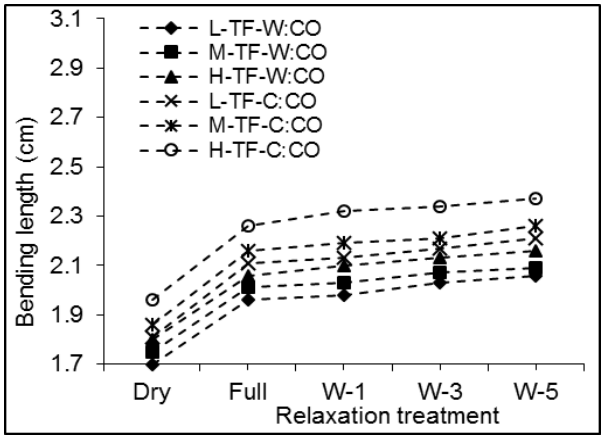

Knitted structure	Fabric TF	Bending length increasing % from dry relax-W5
CO	H-TF	28.64
	M-TF	25.98
	L-TF	25.37
CO-SP	H-TF	31.22
	M-TF	29.63
	L-TF	29.86

Figure 6: Bending lengths of CO fabrics in wale and course directions

Thus, according to the tables given with Figures 5 and 6, bending lengths have increased i.e: increasing the fabric stiffness) with the progressing of treatments. Possible reasons would be that progression of treatments also increases the stitch densities, which results higher bending lengths (stiffness) in both types of knitted structures. Other possible reason is that increasing the restrictions to yarn movements and the yarn compressional forces due to increasing of course and wale densities can restrict the bending of fabric samples. Thus, it can be assumed that as the rigidity and straightness of spandex filaments in the CO-SP yarn structure, the core spun yarns may have higher flexural rigidity values than 100% CO yarns, which can also increase the stiffness properties. Hence, higher thickness of CO-SP single jersey structures may have additional influence on the higher bending lengths and flexural rigidity. Thus, bending length of fabric samples positively correlates to the stitch length $^{-1}$, which is clearly demonstrated by Figures 5 and 6.

Thus, flexural rigidity, which is a mechanical value of the fabric stiffness, has been calculated using the following equation given in ASTMD 1386-96.

$$Flexural\ rigidity\ (mg.cm) = W \times C^3 \quad (1)$$

where W-areal density (mg/cm^2); C-bending length (cm)

Then, flexural rigidity values were determined using equation (1). The results are shown in Figures 7 and 8 in course and wale directions respectively.

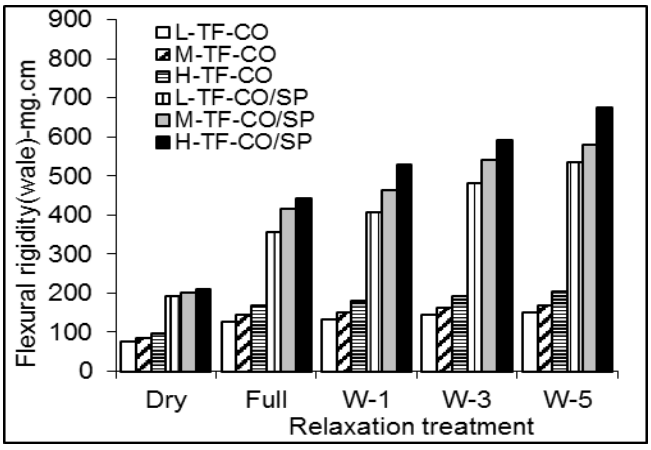

Figure 7: Flexural rigidity variations of single jersey fabrics in wale direction

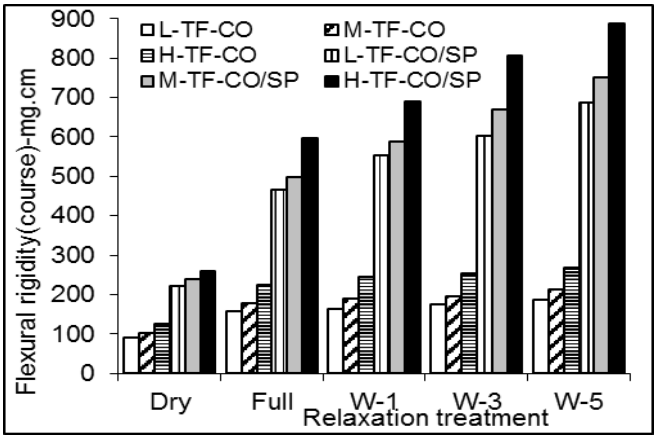

Figure 8: Flexural rigidity variations of single jersey fabrics in course direction

CO-SP single jersey fabrics have given significantly higher flexural rigidity values than CO structures and thus, flexural rigidity of tested samples positively correlate to fabric rightness factor and stitch length^{-1}. Reason could be the higher areal density and bending lengths achieved by CO-SP samples compared to CO structures, as described earlier. Meanwhile, flexural rigidity has increased with progression of treatments. This is especially observed in the case of CO-SP single jersey structures, both in course and wale directions. However, in CO structures, there is no significant increase in flexural rigidity observed after full relaxation.

Air permeability variations

Air permeability of a fabric is defined as the volume of air in cm^3, which is passed in one second through 1cm^2 of the fabric at a pressure difference of 10 mm head of water. This physical property is very important in concern of comfort in clothing.
Figure 9 shows the variations of air permeability of CO and CO-SP single jersey fabrics subjected to relaxation treatments.

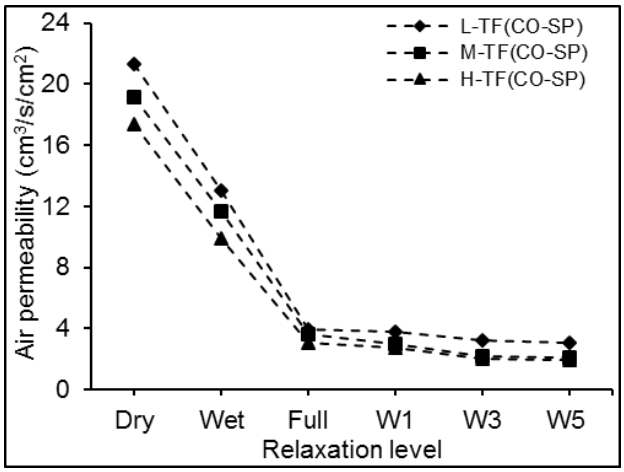

Knitted structure	Fabric TF	Air permeability reducing % from dry relax-W5
CO	H-TF	28.64
	M-TF	25.98
	L-TF	25.37
CO-SP	H-TF	31.22
	M-TF	29.63
	L-TF	29.86

(a) For CO-SP single jersey structures

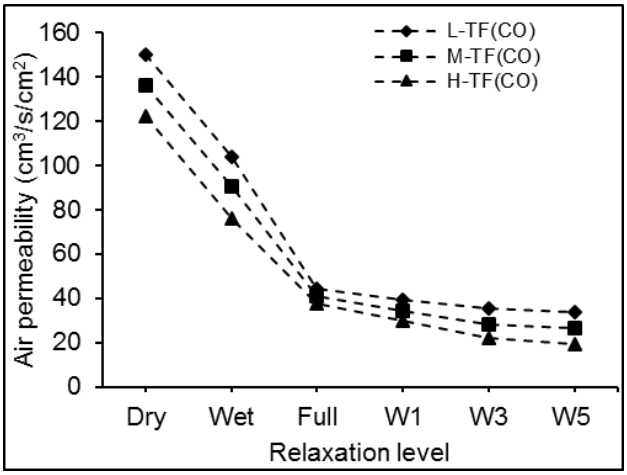

Knitted structure	Fabric TF	Air permeability reducing % from dry relax-W5
CO	H-TF	85.63
	M-TF	80.62
	L-TF	84.28
CO-SP	H-TF	88.74
	M-TF	88.98
	L-TF	88.74

(b) For CO single jersey structures

Figure 9: Air permeability variations of CO and CO-SP single jersey fabrics

The table given with the Figure 2 shows that air permeability reduced with the relaxation treatments. Further, it is very clearly shown that air permeability has drastically decreased from dry relaxation to full relaxation in both knitted structures (as for CO about 70% and for CO-SP about 82%), due to increasing of stitch densities as illustrated in Figure 2, which is resulted of increasing areal density as described previously. Further, air permeability has reduced with progression of laundering treatments due to the same reason, but the rate is significantly lower than dry- to full-relaxation period. Thus, CO single jersey fabrics have shown higher air permeability values than CO-SP single jersey fabrics under the each treatment level because of their lower stitch density variations, which makes higher porosity in the knitted structure, compared to CO-SP single jersey fabrics. Hence, air permeability of single jersey CO and CO-SP knitted structures show a positive correlation to the machine set stitch length (or proportionate to the fabric tightness factor^{-1}). This could be happened due to making more structural spacing in the fabric with lower stitch lengths, which enables for higher air permeability in the fabrics.

Bursting strength variations

Bursting strength variations of CO and CO-SP single jersey knitted fabrics under relaxation treatments are shown in figure 10.

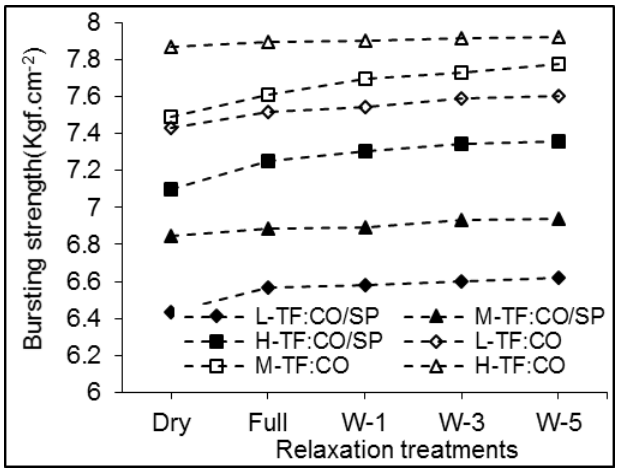

Knitted structure	Fabric TF	Bursting strength increasing % from dry relax-W5
CO	H-TF	0.64
	M-TF	3.79
	L-TF	2.34
CO-SP	H-TF	3.66
	M-TF	1.39
	L-TF	2.89

Figure 10: Bursting strength variations of CO and CO-SP single jersey fabrics

It shows that bursting strength of CO and CO-SP single jersey fabrics positively correlate to stitch length^{-1} of fabric. Because, lower stitch lengths results higher stitch densities as shown in Figure 2, which can bear the three dimensional bursting forces than lower stitch length knitted fabrics. Thus, bursting strength increased with the relaxation of knitted structures during progressing of treatments as the table given with Figure 10, because, stitch configuration changes during relaxation results higher stitch densities, which can bear bursting forces.

Hence, CO single jersey fabrics have shown higher bursting strength values than that of CO-SP single jersey fabrics, even though they have knitted with same machine set stitch lengths and CO-SP showed higher stitch densities as given in Figure 2. Reason could be hypothesized as the modulus and strength of CO-SP yarns can be reduced with repeated tumble drying done at each relaxation stage from full relaxation to W-5. Then, soft segments in polyurethane molecules (from polyols) in spandex filaments may affect by this, because they have lower melting point and very low glass transition temperature (Tg : 190 - 200K) compared to the hard segments of polyurethane molecules (from di-

isocynate). But, this change may not happen with CO fabrics as they have good resistant to heat. Thus, it can be observed a significant increasing of bursting strengths from dry relaxation to full relaxation than during progression of washing treatments (W-1 to W-5). Because, structural parameters increase rapidly in this period and results higher stitch densities for both knitted structures as shown in figure 2 [Herath and Kang, 2008)]. Therefore, the increasing stitch densities would have not much significantly affected on the variations of bursting strength of CO-SP single jersey fabrics, but the effect of repeated washing and tumbler drying have given very significant influence on it.

Multiple regression models and ANOVA analysis

Based on the multiple regression technique and ANOVA analysis, mathematical models for flexural rigidity, air permeability and bursting strength variations of CO and CO-SP single jersey fabrics were established under 95% significant level. In establishing these models, data obtained in full relaxation, after 1st(W1), 3rd (W3) and 5th (W5) machine wash cycles were used. Table 4 and 5 show the multiple regression model and ANOVA analysis for flexural rigidity variations of CO and CO-SP single jersey fabrics.

Table 4: Multiple linear regression model for flexural rigidity of CO-SP plain fabrics

Regression model for full relaxation to 5th washing cycle

Direction	variables entered	Correlation model	Pr>F	R^2
Wale	M, t	Y = -779.683+2.355M+547.901t	<0.0001	0.9740
Course	M, t	Y = -1051.037+3.52M+574.062t	<0.0001	0.9630

Note: Y- Flexural rigidity (mg.cm); M-weight/area (g/m²); t-thickness (mm)

ANOVA summary for regression model

Direction	Variable	Standard error	Standardized estimate	t value	Pr> $\lvert t \rvert$	F value
Wale	Intercep	60.931	0	-12.79	<0.0001	228.5
	M	0.279	0.664	8.453	<0.0001	
	t	116.419	0.370	4.706	0.001	
Course	Intercep	217.67	0	-8.067	0.004	154.3
	M	0.828	0.819	7.284	0.005	
	t	205.49	0.246	2.188	0.116	

Note: df: regression=2; residual=12: $F_{0.05}$=3.89

Table 5: Multiple linear regression model for flexural rigidity of CO plain fabrics

Regression model for full relaxation to 5th washing cycle

Direction	variables entered	Correlation model	Pr>F	R^2
Wale	M, t	Y = -393.853+1.48M+398.64t	<0.0001	0.9890
Course	M, t	Y = -635.132+2.4M+565.776t	<0.0001	0.9940

Note: Y- Flexural rigidity (mg.cm); M-weight/area (g/m²); t-thickness (mm)

ANOVA summary for regression model

Direction	Variable	Standard error	Standardized estimate	t value	Pr> $\|t\|$	F value
Wale	Intercept	21.292	0	-18.49	<0.0001	564.2
	M	0.116	0.638	12.72	<0.0001	
	t	49.236	0.406	8.097	<0.0001	
Course	Intercept	25.537	0	-24.87	<0.0001	936.9
	M	0.140	0.671	-17.19	<0.0001	
	t	59.052	0.374	9.581	<0.0001	

Note: df: regression=2; residual=12: $F_{0.05}$=3.89

Table 4 shows very strong correlations (R^2>0.96) of flexural rigidity to weight density and thickness values in both wale and course directions of CO-SP plain fabrics. Predicted models are highly significant (p<0.0001) at 95% significant level. According to "standardized estimate" data, both weight density and thickness give positive effect on flexural rigidity of both directions, but weight density effect is at least two times higher than that of thickness.

According to the values given in Table 5, CO plain fabrics also show very strong correlation in both wale and course directions (R^2>0.98). Predicted models are highly significant (p<0.0001) at 95% significant level, as indicated by their F values. Thus, according to "standardized estimate" data, weight density effect is higher than that of thickness on flexural rigidity of CO plain fabrics in concern of both wale and course directions. Hence, weight density and thickness give positive effect in all cases.

Tables 6 and 7 show the multiple regression model and ANOVA analyses for air permeability variations of CO and CO-SP single jersey fabrics.

Table 6: Multiple linear regression model for air permeability for CO-SP single jersey fabrics

Regression model for full relaxation to 5th washing cycle

Number of variables	variables entered	Regression model	Pr>F	R^2
2	M, t	Y = 54.283-0.175M+7.172t	<0.0001	0.9190

Note: Y-air permeability ($cm^3/cm^2/s$); M-weight/area (g/m^2); t-thickness (mm)

ANOVA summary of regression model

Variable	Estimated coefficients	Standard error	Standardized estimate	t value	Pr> $\|t\|$	F
Intercept	54.283	5.141	0	10.56	<0.0001	68.1
M	-0.175	0.024	-1.039	-7.44	<0.0001	
t	7.172	0.982	0.102	7.30	0.479	

Note: df: regression=2; residual=12 : F0.05=3.89

Table 7: Multiple linear regression model for air permeability of CO single jersey fabrics

Regression model for full relaxation to 5th washing cycle

Number of variables	variables entered	Regression model	Pr>F	R^2
2	M, t	Y = 949.78+0.423M-1402.15t	<0.0001	0.9780

Note: Y- air permeability ($cm^3/cm^2/s$); M-weight/area (g/m^2); t-thickness (mm)

ANOVA summary of regression model

Variable	Estimated coefficients	Standard error	Standardized estimate	t value	Pr> $\|t\|$	F
Intercept	949.78	40.434	0	23.49	<0.0001	68.2
M	0.423	0.221	0.140	1.913	0.08	
t	1402.15	0.930	-1.098	-14.99	<0.0001	

Note: df: regression=2; residual=12: F0.05=3.89

According to the Table 6, air permeability of CO-SP single jersey structures have shown higher and very stronger correlation to weight density and thickness values (R^2>0.91). But, according to "standardized estimate" data, weight density gives higher and negative effect on air permeability, but the effect given by fabric thickness is lower and positive

Table 7 shows a very strong multiple regression model on air permeability (R^2>0.97) with the variables such as areal density and fabric thickness. According to "standardized estimate" data, fabric thickness gives very strong positive effect, but areal density shows comparatively very much lower positive effect on air permeability of CO single jersey fabrics.

Tables 8 and 9 show the multiple regression model and ANOVA analysis for bursting strength variations of CO and CO-SP single jersey fabrics.

Table 8: Multiple linear regression model for bursting strength of CO-SP single jersey fabrics

Regression model for full relaxation to 5th washing cycle

Number of variables	variables entered	Regression model	Pr>F	R^2
2	M, t	Y = 4.737+0.006M+4.619t	<0.0001	0.8690

Note: Y-bursting strength (Kgf/cm^2); M-weight/area (g/m^2); t-thickness (mm)

ANOVA summary of regression model

Variable	Estimated coefficients	Standard error	Standardized estimate	t value	Pr> $\|t\|$	F
Intercep	4.737	0.295	0	16.038	<0.0001	39.7
M	0.006	0.0013	0.807	4.539	0.001	
t	4.619	0.564	1.455	8.185	<0.0001	

Note: df: regression=2; residual=12: F0.05=3.89

Table 9: Multiple linear regression model for bursting strength of CO single jersey fabrics

Regression model for full relaxation to 5th washing cycle

Number of variables	variables entered	Regression model	Pr>F	R^2
2	M, t	Y = 6.78+0.015M-2.649t	<0.0001	0.8630

Note: Y-bursting strength (Kgf/cm²); M-weight/area (g/m²); t-thickness (mm)

ANOVA summary of regression model

Variable	Estimated coefficients	Standard error	Standardized estimate	t value	Pr> $\|t\|$	F
Intercept	6.78	0.394	0	17.212	<0.0001	37.7
M	0.015	0.002	1.300	7.178	<0.0001	
t	-2.649	0.911	-0.527	-2.908	0.013	

Note: df: regression=2; residual=12: F0.05=3.89

According to the Table 8, bursting strength of CO-SP single jersey fabrics have very strong correlation (R^2>0.86) with areal density and thickness, which gives negative and positive effects on bursting strength respectively. According to "standardized estimate" data, thickness can give higher effect than areal density on bursting strength of CO-SP single jersey fabrics.

In the case of bursting strength of CO single jersey fabrics, areal density and thickness are also given strong correlation on it as given in Table 9 (R^2>0.86). But, according to the 'standard estimate data", the effect of weight density and thickness are positively and negatively affecting on bursting strength respectively. Thus, this predicted models given in Tables 4, 5, 6, 7, 8 and 9 are highly significant at 95% significant level.

CONCLUSIONS

Significant structural changes occur during relaxation of knitted stitches in the single jersey fabrics due to the treatments done and it rapidly increases with progression of treatment. Due to this, structural spacing, which correlates to the machine set stitch lengths, significantly reduced with during treatments. CO-SP single jersey fabrics gave lower structural spacing than that of CO fabric, even though both have knitted with same machine set stitch lengths. Thus, steeper structural spacing reductions reported from dry relaxation to full relation compared to further treatment levels. Stitch density variations showed the same tendencies in all relaxation levels with both CO-SP and CO single jersey structures.

Fabric thickness has increased during relaxing the knitted stitches and it has showed the progressive results with the high level of treatments. CO-SP single jersey fabrics showed significantly higher fabric thicknesses than CO fabrics under same machine set stitch lengths. Fabric thickness has given negative correlation to the stitch lengths. Similar types of tendencies can be given by the variations of areal densities, fabric stiffnesses and flexural rigidity of both CO-SP and CO single jersey structures during treatments. Thus, fabric stiffness is higher in course direction than in wale direction in both fabric types

under the treatments. Thus, bursting strengths of single jersey fabrics, which is progressively increased with higher level of treatments, reported the higher values in CO-SP fabrics compared to CO fabrics under the treatments and it is negatively correlates to stitch length.

Fabric stiffness, flexural rigidity, air permeability and bursting strength of CO-SP and CO single jersey fabrics showed the strong correlations with areal density and fabric thickness of the fabric and all the considered physical properties are significantly influenced by the machine set stitch lengths, the relaxation level and material type.

REFERENCES

1. Herath C. N. and Kang B. C. (2008), Dimensional stability of Core spun Cotton/spandex Single Jersey Fabrics under Relaxation, *Textile Research Journal*, 78(3): 200-216.

2. Marmarali, A.B., (2003), Dimensional and physical properties of Cotton/Spandex Single Jersey Fabrics, *Textile Research Journal,* 73(1): 11-14.

3. Sharma, I. C., Ghosh, S. and Gupta, N. K., (1985), Dimensional and physical characteristics of Single Jersey Fabrics, *Textile Research Journal*, 55: 149-156.

4. Hepworth, B., (1982), The dimensional and mechanical properties of plain weft knits, *Knitting International*, 1: 33-37.

5. Mavruz, S. and Ogulata, R. T. (2010), Tagushi approach for the optimization of bursting strength of knitted fabrics, *Fibers & Textiles in Eastern Europe*, 18(29):78-83.

6. Ertugrul, S. and Ucar, M. (2000), Predicting bursting strength of cotton plain knitted fabrics using intelligent techniques, *Textile Research Journal*, 70(10): 845-851.

A Study on Impact of Visual Merchandising on Consumer Buying Behaviour in Clothing Retail Stores

N.H. Wanniachchi, W.V.L. Kumara*

Department of Textile and Apparel Technology, Faculty of Engineering Technology, The Open University of Sri Lanka, Nawala, Nugegoda, Sri Lanka.

*Corresponding Author: email: wvkum@ou.ac.lk, Tele: +94776385130

Abstract *– This paper presents a study conducted to identify the impact of visual merchandising elements, on consumer buying behaviour, to identify the most appealing visual merchandising elements. The purpose of visual merchandising is to attract, engage and motivate the customer towards making a purchase, where it creates an impact on the consumer buying behaviour.*

In this study, visual merchandising elements are categorised into two sections, exterior and interior elements for analysis and conclusions. Exterior elements are exterior signs, marquees, entrance, window displays. Interior elements are mannequins, colours, lightings, cleanliness, music, interior signs, space & layouts, creative display, video display, focal points, and fragrance.

To study the impact of above-mentioned elements, four leading clothing retail shops are identified in the areas of Kohuwala, Piliyandala, and greater Colombo. Two from those four retail stores are branded stores and other two are departmental stores. This has been done to get more realistic or representative sample of consumers as the data source. First, available visual merchandising elements in each store were identified and recorded. Primary data were collected from customers entering the store. Fifty customers from each store were randomly picked and given the questionnaire. The questionnaire was designed to collect general information (section 1) such as age group and gender. Section 2 dealt with how visual merchandising elements impact on them. The Likert scale is used to identify the level of impact from "strongly agree" to "strongly disagree". Twelve elements, both interior and exterior, were considered for the questionnaire.

First, primary data were analysed to conclude, whether visual merchandising elements have an impact on the sample population. Primary data were analysed using spider web diagram. Primary data, a total of 200 samples was analysed as one cluster first, and then clusters were analysed gender wise to find out how male or female customers are influenced by visual merchandising and finally, age group wise clusters were taken to see which age group has a greater influence over visual merchandising elements. To draw the spider web diagram only the strongly agree and agree responses were considered. Then the highly influenced elements were identified in different clusters as well as on a total. Then compare the strategies use by international branded stores, when using these identified highly influencing elements. Suggest those strategies to the selected retail stores to improve the impact of the visual merchandising element and draw more customers into the store.

From the collected data it was showed that there were no any disagreed and strongly disagreed responses from the total sample population. It clearly shows that the selected visual merchandising elements have a positive impact towards consumer buying behaviour. 96% of the sample population accepted they believe those elements had influenced them to attract, engage or motivate them to experience the merchandise assortments. From the study, it was found that window display and mannequins are the highly influencing elements and also colour combinations, lighting, use of music and creative display also has a great influence over consumer buying.

Keywords: Visual merchandising, Consumer buying behaviour, Visual merchandising elements, Window display, Mannequins

1. INTRODUCTION

1.1 Project Introduction

According to (Matthysz, 2003), Visual merchandising involves everything the customer sees in approaching the store and after entering it. This includes the exterior appearance of the store, the store sign, display windows, interiors décor, store layout, fixturing, lighting, and they way the merchandise is presented and displayed within the store. Visual merchandising also includes activities that appeal to the customer's senses other than the visual, such as music or fragrance.
Until recently, the activity was simply called display. However, visual merchandising is much broader than display, which is the impersonal visual presentation of merchandise and props.
Visual merchandising, or visual presentation, is used to communicate fashion, value and quality attributes of a store to its prospective customers.

The purposes of visual merchandising are to educate the customer, to enhance the stores' image, and to encourage multiple sales by showing apparel together with accessories.
Since the ultimate goal of visual merchandising and of retailing is to get the customer to buy, visual merchandising must entice the consumer into the store, effectively present the fashions the store has to offer, and show the customer how to wear and access them within the context of fashion trends. With increased competition, stores are trying to create more exciting, aggressive visual presentations.

According to (Khaniwale, 2015), Consumer behaviour involves the study of individuals and the method they employ to choose, utilise, and set out products and services to fulfil their wants and the effect that these methods have on the consumer and the society as a whole. Consumer behaviour refers to all the thoughts, feelings and actions that an individual has or takes before or while buying any product, service or idea. Buyer behaviour is the concept which answers what, why, how, when, and where an individual makes a purchase.

A few international researchers have contributed to the field by exploring the visual merchandising techniques which cause the customers impulsive buying, but still there is more to be determined. However, considerable research studies have not been undertaken on the impact of visual merchandising on consumers buying behaviour in clothing retail outlets of Sri Lanka. Hence, the purpose of this study is to identify the influence of visual merchandising techniques on consumer buying behaviour in Clothing Retail Stores.

1.2 Problem Identification

According to the report "The Report: Sri Lanka 2016" published by Oxford Business Group indicates retail becomes one of the Sri Lanka's fastest growing sectors. The retail industry in Sri Lanka has emerged as one of the most dynamic and rapidly growing industries today. Clothing retail industry is a very volatile one. There is a high degree of competition among the clothing retail market and most of the clothing retailers are fighting to attract customers as well as to stand out from the rest and to be the best clothing retail chain in the country.

In Sri Lanka, clothing outlets use different types of visual merchandising elements to attract the customers, but comparatively apply less of advance elements, rapidly used in the world. Moreover, some of the retail stores apply these elements without proper mechanism and standards, thereby not achieving the expected results. This leads to loss of facilities with those elements. On the other hand, customers do not perceive the effect of the applied element, thereby level of sales expectation is not realised.

1.3 Aim & Objectives

1.3.1 Aim

The aim of this research is to study the influence of visual merchandising elements on consumer buying behaviour by focusing on selected clothing retail stores in Sri Lanka, to identify the highly influential visual merchandising elements and then comparing the results with that of international retails stores, to decide on improvements can be made to attract more customers in Sri Lankan context.

1.3.2 Objectives

- To study on the highly influential visual merchandising elements applied in international branded clothing retail stores.
- To explore the elements of visual merchandising used in clothing retail stores in Sri Lanka in comparison to the elements used in international retail stores.
- To study the impact of visual merchandising on consumer buying behaviour.
- To analyse the highly influential visual merchandising elements on consumer buying behaviour in Sri Lanka.

2. LITERATURE SURVEY

2.1. Visual merchandising elements

Visual merchandising techniques can be divided as follows;

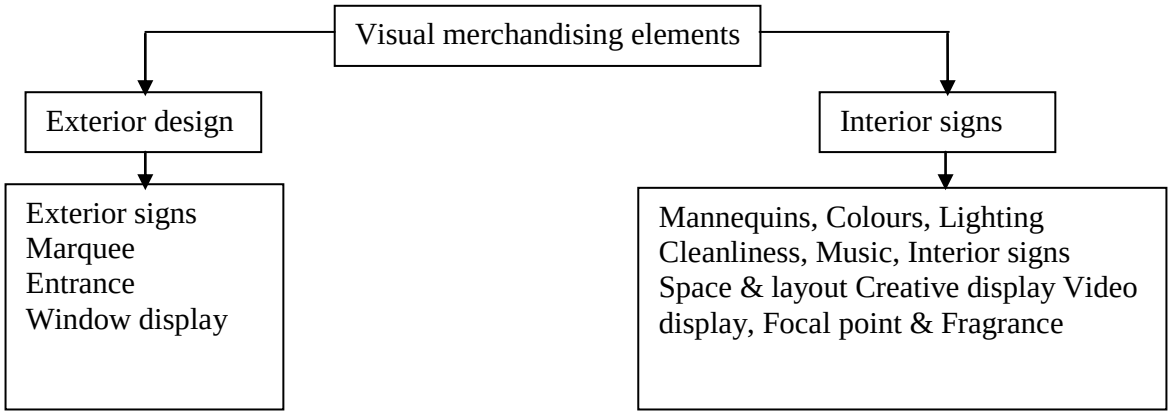

Figure 1: Visual Merchandising Elements

2.2 Past research findings

Saini, C., Gupta R., Khurana I. (2015) have studied the effect of Visual Merchandising on consumers' impulse buying behaviour and found out the key elements of Visual Merchandising contributing the most for impulse buying. The study found that visual merchandising practices certainly influence customers' buying behaviour and leads to Impulse buying as well. The results suggest that the themes that linked most strongly to purchase intention were: merchandise colours, presentation style, awareness of fixtures, pathfinding, sensory qualities of materials and lighting.

Kaur, A. (2013) proved that there was a relationship between customers' buying behaviour and in-store form/mannequin display, promotional signage and window display. The study also provided insights about types of visual merchandising that can influence customers' buying behaviours. Three most important factors of visual merchandising namely attractiveness of window display, innovative assortments and cleanliness and neatness of store/ store environment have been identified. The conclusion of his research is that the visual merchandising has a direct relation with the sales performance. Customers get attracted, hence increasing the store's footfall, which ultimately has a positive impact on the sales figures.

Jadhav R.A., Chaudhary P.V. (2014) research study was focused on determining the important factors of visual merchandising which influence consumers' perceptual process, buying behaviour and in-store promotion activities. Various visual merchandising techniques had been considered and studied their impact on the buying behaviour of the customers and also tried to understand and explain the relationship between impulse buying and visual merchandising. Visual merchandising served as a significant influence on the retail experience and the shoppers' decision-making process. It provides a competitive advantage and helps in building the overall image of the store.

Madhavi, S., Leelavati T.S (2013) presented the results of an initial investigation on "visual merchandising" and its effects on purchasing behaviour. The scope of the study was to study the influence of visual merchandising, especially the one related to the shop-windows, on consumer buying behaviour according to store attributes most valued by consumers. The themes that linked most strongly to purchase intention were: merchandise colours, presentation style, awareness of fixtures, pathfinding, sensory qualities of materials and lighting. The study proved sufficient evidence that retailers can utilise visual merchandising to increase the desirability of products and to help customers to be aware of the products as well as to create favourable attitudes.

Makhal, A.B (2015) found that there is an interaction or relationship between the type of shopper and the visual merchandising elements. The Estimated Marginal Means for both fixed factors confirm the same. The Posteriori Tests reveal that in terms of scores, shoppers have given maximum importance to Set 3 elements-music, aroma, arrangement of merchandise, aisle space, lighting and store cleanliness; followed by Set 2 elements- flooring and in-store signage; and lastly Set 1 elements- wall color/texture and store exterior; in respect of lifelong customer loyalty.

3. METHODOLOGY

3.1 Procedure and the work plan

The proposed methodology is shown in Figure 2. First, a comprehensive literature survey was carried out. Then select data sources, data collection methods and the data analysis methods were decided.

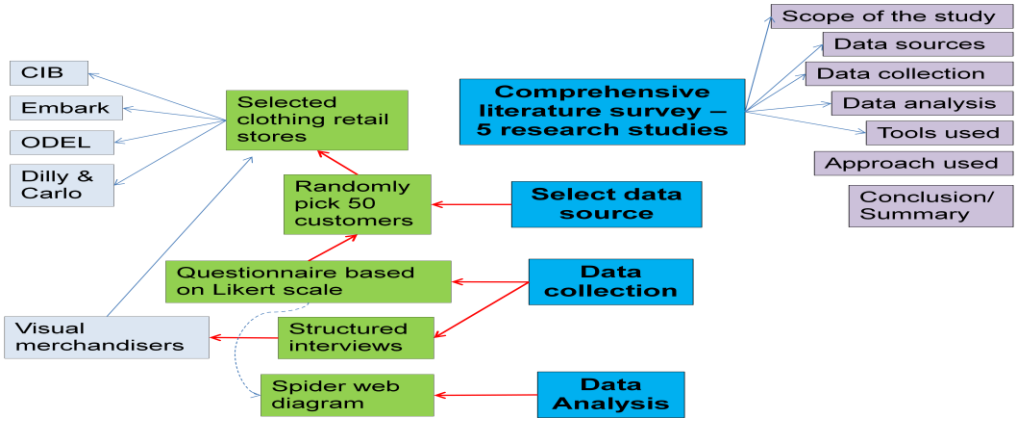

Figure 2: Proposed methodology in sequence

To carry out the research, four retail stores were selected, namely Dilly & Carlo outlet in Flower road, Embark outlet in Dickman road, ODEL outlet in Kohuwala and CIB outlet in Piliyandala.

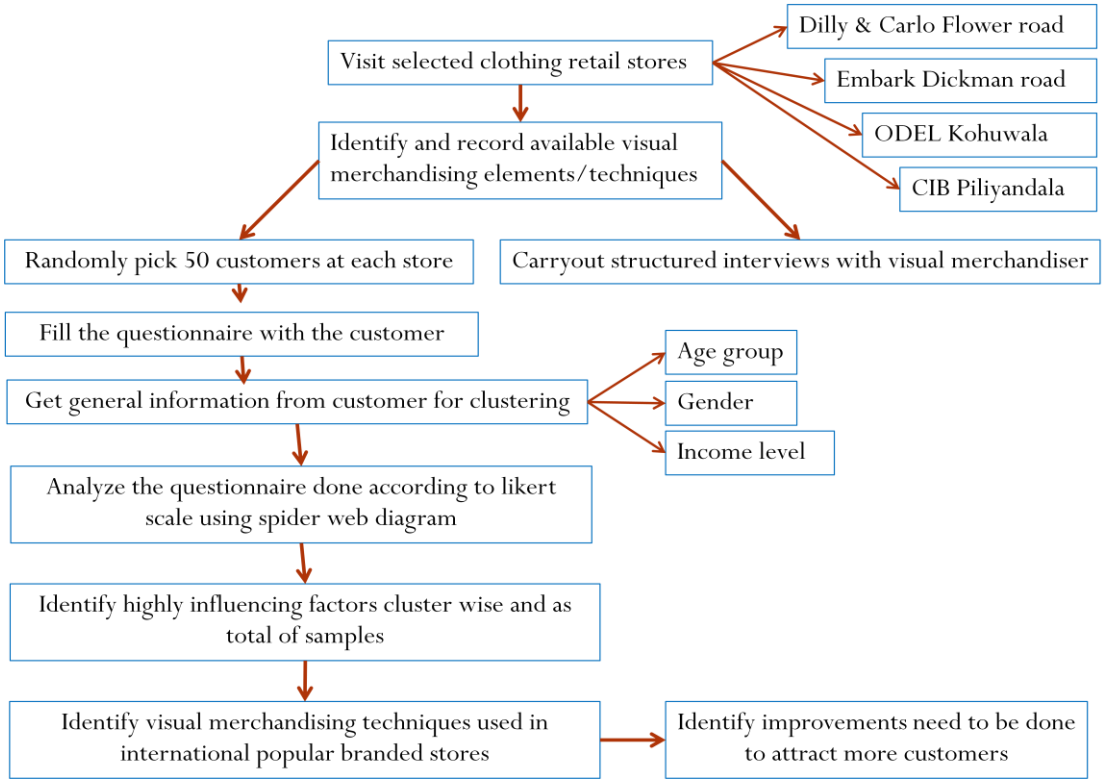

Figure 3: Comprehensive work plan for research project

3.2 Questionnaire for Customers

As per the work plan, first visit selected outlets and record the present aspect of visual merchandising elements, then two types of data sources were selected as primary and secondary data. For primary data fifty walk-in customers randomly picked, and gave the questionnaire to be filled. The purpose of the data collection and the technical terms in the questionnaire were explained to them with suitable photographs.

Dear Sir/Madam,

I am, Nadeesha H. Wanniachchi, an undergraduate student in Apparel production and Management in Open University, conducting a research survey on study of the impact of visual merchandising on consumer buying behaviors as a part of partial fulfillment of my degree program. I kindly request you to spare few minutes of your valuable time in filling the following questionnaire. Your response in this regard shall be great input for the act of which I shall thankful to you.

(This will only be used in support of above mentioned research paper)

Guidance to Complete:

Please mark your selected answer with (✓) in the given chart and write the specified answer in given space.

Name (Optional) : .....

i. **Name of the Store**

a. ODEL ☐ c. Embark ☐

b. Dilly & Carlo ☐ d. CIB ☐

ii. **Gender** :

a. Male. ☐ b. Female. ☐

iii. **Age** :

a. 18 - 24 years ☐ c. 35 - 44 years ☐

b. 25 - 34 years ☐ d. Above 45 years ☐

Mark your response (√) in the appropriate column;

Questions	Strongly Agree	Agree	Neutral	Disagree	Strongly Disagree
Exterior Design					
1. You choose to enter in to the store because creative window arrangement in store front, take your attention, create interest & invite you into the store.					
2. The display of signs in front of the store would provide information about the product items and it attracts you into the store.					
3. The arrangement of the entrance of the store would positively affect your impression about the store.					
Interior Design					
4. New clothing designs displayed on dummies would make an idea about the outfit which helps to select the items.					
5. Product items placed according to different color combinations take your attention immediately and allow you to find items more easily.					
6. The use of lights in different brightness to decorate the store would attract to the items which are clearly seen and swing your mood towards buying.					
7. Cleanliness and neatness of the store would make positive impression about the products.					
8. The use of music in the store tends you to spend more time and make choices freely.					
9. The signs of the special offers and brands displayed inside the store would make positive impact in your mind and tend to buy more items.					
10. A good space and proper layout inside the store would make a comfortable environment to you.					
11. The way of presenting the items and decorations of the store would increase the interest to purchase.					
12. Video displayed in digital screens & walls helps you to get information about new arrivals & promotions.					

Figure 4(a): The designed questionnaire

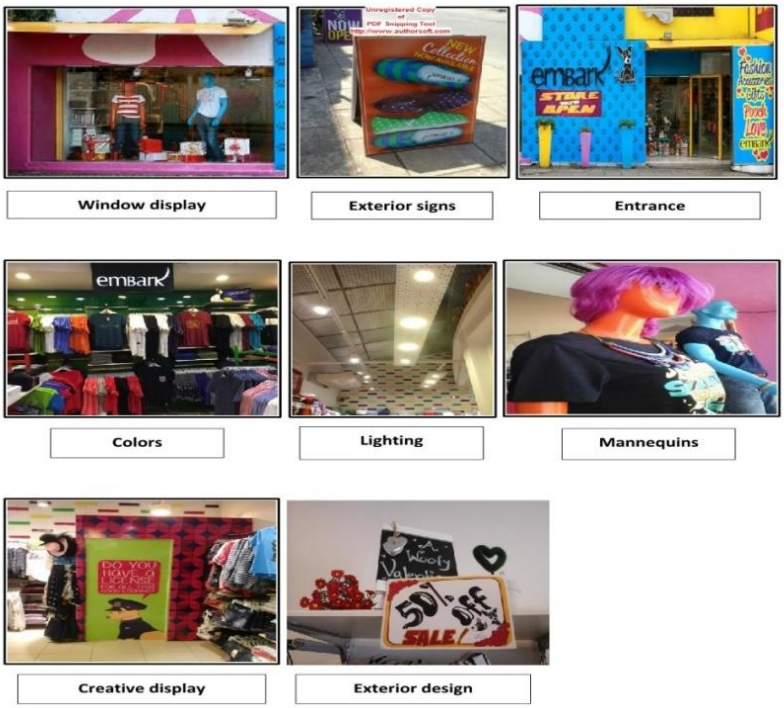

A total of two hundred samples were collected and the collected data was analysed using spider web diagram. A spider chart is a graphical method of displaying multivariate data in the form of a two-dimensional chart of three or more quantitative variables represented on axes starting from the same point. In a spider chart, a point near the edge represents high value and a point closer to centre on any axis indicates a lower value.

Figure 4(b): Visual aids for the designed questionnaire

4. RESULTS & DISCUSSION

4.1 Visual merchandising elements in selected shops

Available visual merchandising elements were identified and recorded.

- Exterior signs

The purpose of the signs is to gain customer awareness and announce the store identity. There are promotional, directional, location and informational signs.

Figure 5: Exterior signs- Informational & different themes

- Marquee

A special type of signs is used to display the name of a store. Leather, wood, metal or plastic material used.

Figure 6: Marquee applied in stores

- Entrance

Important to attract customers from visual appeal. Straight, arcade and angle store front designs are different types.

Figure 7: Entrance - Straight Store & Angled front

- Window display

Get attention, create interest and invite people to the store. They are regularly updated to show the latest products in the store. Enclosed, open back, corner, showcase, angled and semi-enclosed are some of the window display types.

Figure 8: Enclosed, Semi- Enclose & Live model window displays

- Mannequins

Essential for enhancing the appeal of the clothing by showing how it looks when put on. Realistic, semi-realistic, abstract, semi-abstract, headless and three-quarter mannequins are some types that are frequently used.

Figure 9: Mannequins - Abstract & Semi-Realistic

- Colours

The first element, which consumers respond in selecting or rejecting a garment, is colour. Warm, cool and neutral are the three main colour categories. According to the season, colour combinations change.

Figure 10: Multiple Colours & Light to dark colour arrangements

- Lighting

Use to draw attention to a part of the area or a specific item in the display or to coordinate parts of the total area. Soft lighting creates an intimate and inviting space, while bright lighting creates a modern feel. Floodlights, revolving, flashing, and spotlights are commonly used types.

Figure 11: Different lighting types used at stores

- Interior signs

Brand identification of specific products, identity classification of products, offer direction to various departments, and announce upcoming events and providing information about product benefits are some common purposes of using interior signs.

Figure 12: Different interior signs

- Space & Layout

It represents how effectively the retailer utilises its space. The objectives of store design are to guide the customer around the store and entice increase of purchase, to create a balance between sales and shopping space, to create an effective merchandising presentation and use multi-level to provide sense and variety.

Figure 13: Different sections in a store

- Creative display

According to seasonal themes creating different displays & arrangements and use of different folding and hanging methods are categories of the creative display. Props and fixtures are commonly used

Figure 14: Seasonal Displays and Folding & Hanging methods

- Focal point

A focal point is a place that peoples' eyes will immediately focus on when they first look at the display. Creating an attractively highlighted area with mannequins, accessories and attractive designs is important.

Figure 15: Different focal points

- Cleanliness

The cleanliness of the store and items is the very important. Maintain shop floor and fit on rooms and racks and other fixtures in a cleanly manner.

- Music

Western classical slow music played except at CIB. Background music makes customers tend to spend more time and make choices freely.

- Fragrance

For fragrance air fresheners are used.

4.2 Results of customer base analysis

Total responses

Total responses were analysed to see the impact of visual merchandising elements on consumers. Below graph shows 96% of the total responses are either agree or strongly agree that visual merchandising elements impact their buying behaviour.

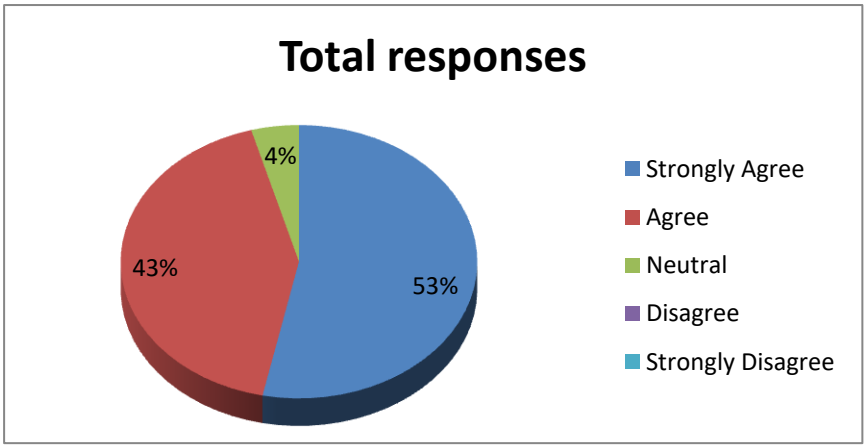

Figure 16: Analysis of total responses from the sample

Gender information

Gender information graph shows, that 72% of the sample responses are on female consumers and only 28% of the male.

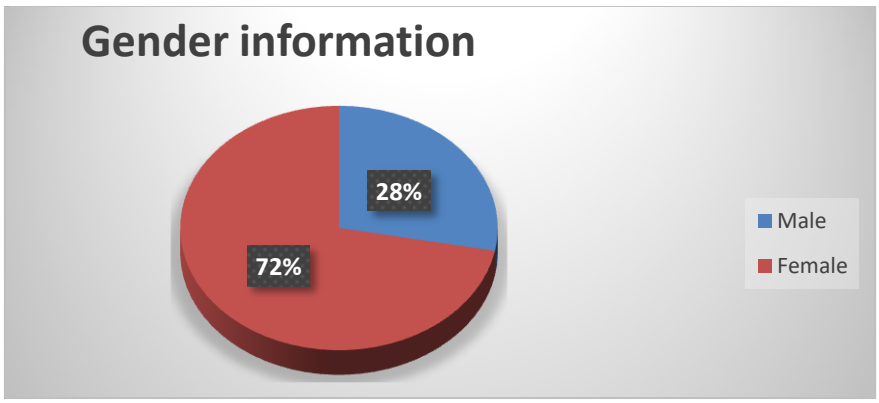

Figure 17(a): Analysis of gender information of the sample

Age group information

Age group information graph shows that 72% of the consumers' belong to the age group 25 - 44 and majority is in the age group 25-34.

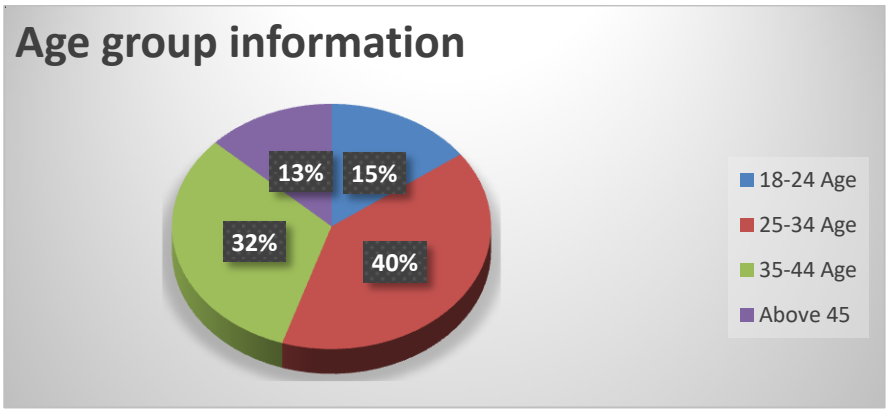

Figure 17(b): Analysis of Age group information of the sample

4.3 Results of customer questionnaire analysis

Total responses

Responses given to the questionnaire by the customers from all the four outlets is given in the table below;

Table 1: Total responses of the sample of 200 customers from all the four outlets

Techniques	Strongly agree	Agree	Neutral	Disagree	Strongly Disagree
Window display	162	38	0	0	0
Color combinations	155	45	0	0	0
Mannequins	151	49	0	0	0
Lighting	125	75	0	0	0
Cleanliness	108	92	0	0	0
Creative display	108	92	0	0	0
Exterior signs	102	98	0	0	0
Entrance	93	104	3	0	0
Interior signs	87	113	0	0	0
Use of music	66	134	0	0	0
Space & Layout	55	84	51	0	0
Video display	8	47	45	0	0

There were no any "disagree" and "strongly disagree" responses from the total of 200 customers randomly picked at each selected store. Above data were plotted in a spider web diagram to clearly identify the highly influential elements of visual merchandising.

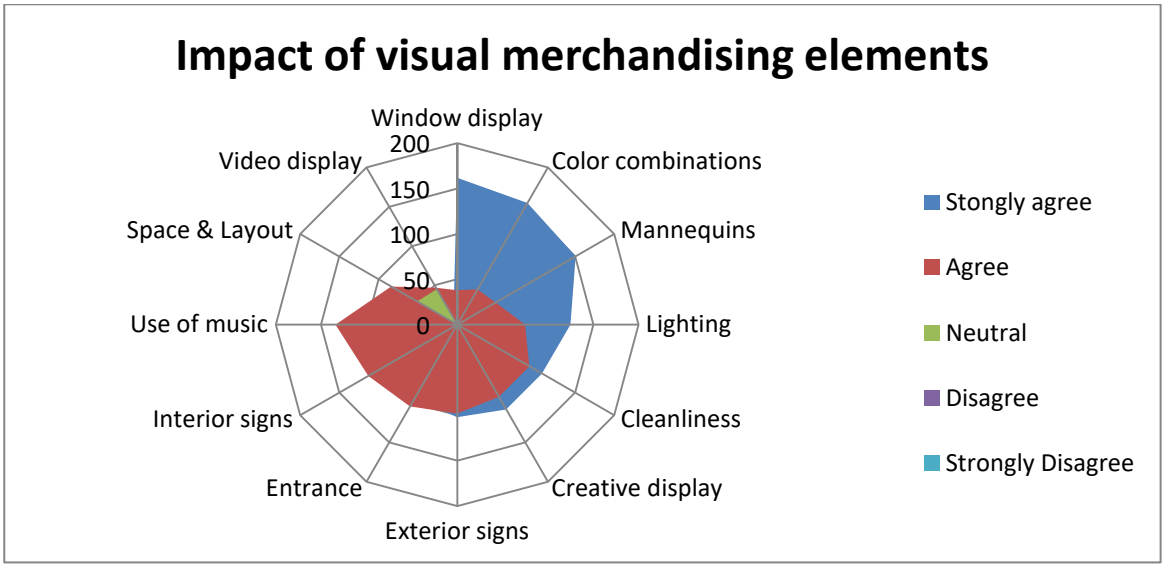

Figure 18: Spider web diagram - number of responses on each visual merchandising element

This graph clearly indicates window display, colour combination and mannequins have the highest impact on consumer buying behaviour and lighting and use of music also have a greater impact too.

Store wise analysis

ODEL

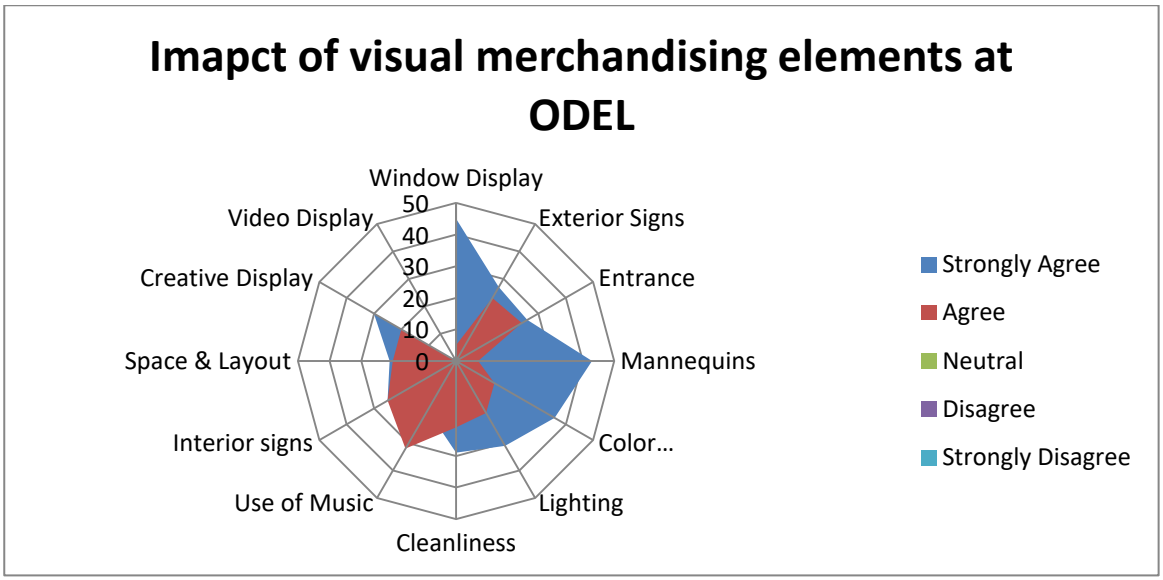

Figure 19: Spider web diagram - number of responses on each visual merchandising element at ODEL

At ODEL window display, mannequins and creative display have the highest impact. And also colour combination, lighting and use of music plays greater impact too.

Embark

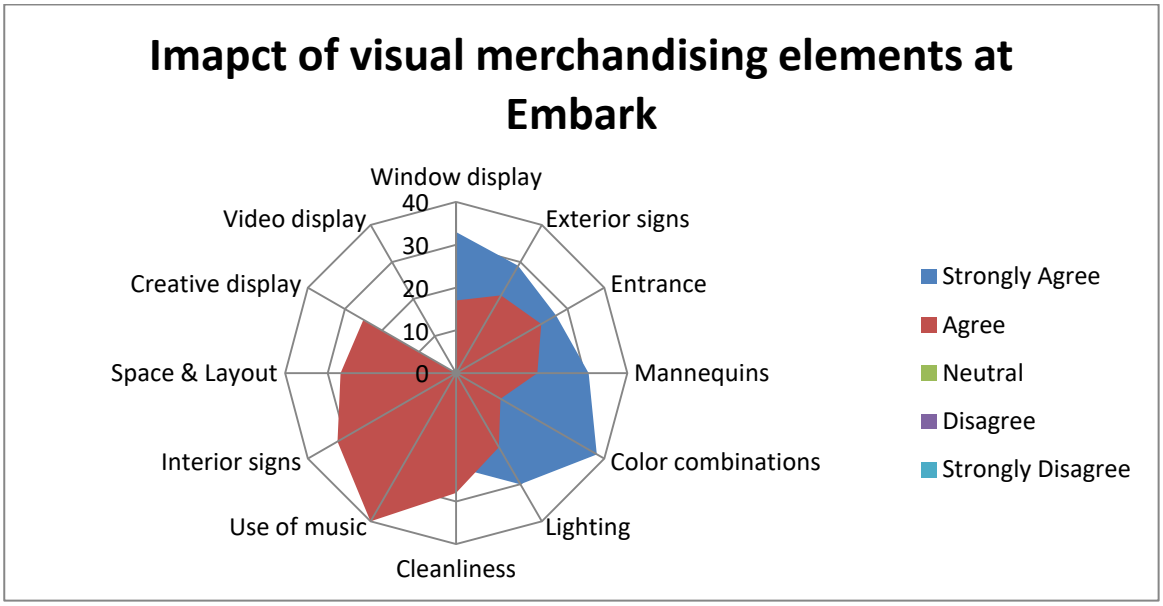

Figure 20: Spider web diagram - number of responses on each visual merchandising element at Embark

At Embark window display, colour combination and use of music have the greatest impact on consumers'. And also lighting, interior signs and entrance have a greater impact too.

Dilly and Carlo

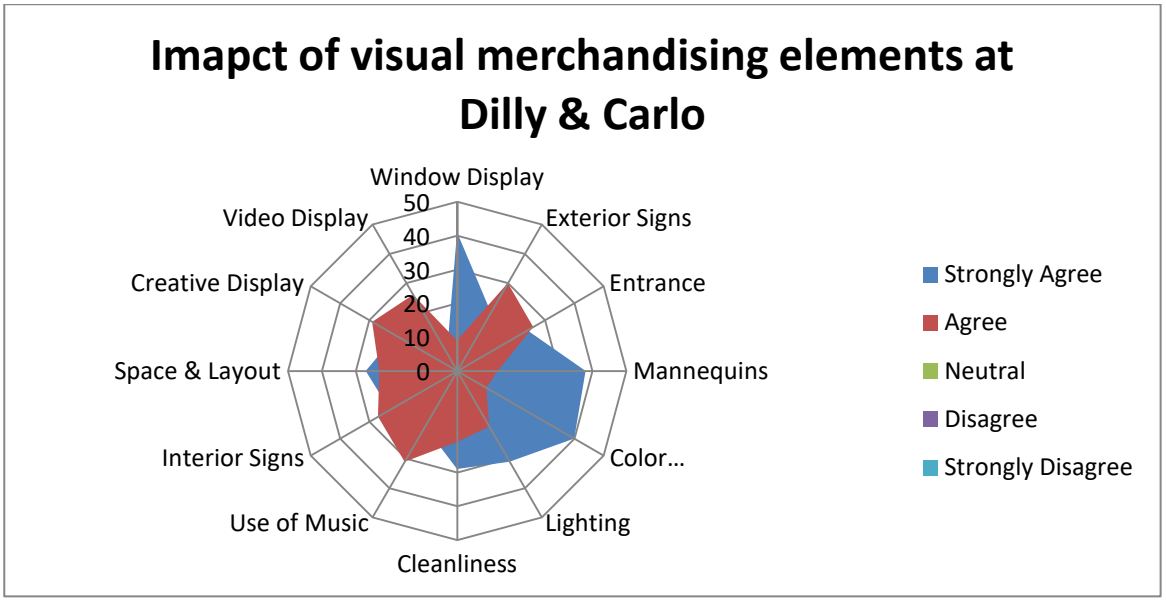

Figure 21: Spider web diagram - number of responses on each visual merchandising element at Dilly & Carlo

At Dilly & Carlo window display, mannequins and colour combination have the highest impact on consumers'. And also lighting, exterior signs and use of music have a greater impact too.

CIB

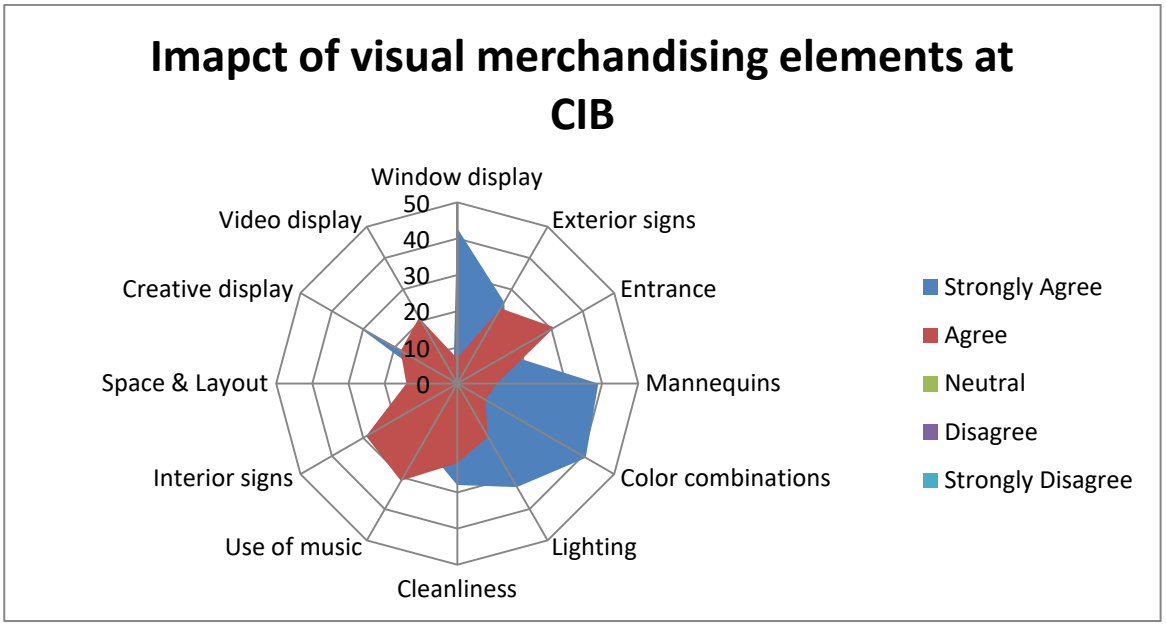

Figure 22: Spider web diagram - number of responses on each visual merchandising element at CIB

At CIB window display, colour combinations and mannequins have the greatest impact on the consumers'. And also lighting, use of music, entrance and interior signs plays a greater impact too.

5. RECOMMENDATIONS

The highly influential or effective visual merchandising elements are window display, mannequins, colour combination, use of music and creative displays. Compared with international branded stores, following recommendations can be made for Sri Lankan retail stores.

- Some creative window displays are arranged without using dummies. It is a quite different as customer attention is directly taken only to the clothing but the dummies.

Figure 23: Mirror used & without dummies window display

- Digital Screens are considered as one of the most effective methods used in internationally mostly in major cities for effective communication with potential customers.

Figure 24: Digital screen on window and inside

- It is evident that most customers can be inspired with the creative lighting arrangement. Some of the decorative lightings used in international stores shown in the picture, which has reflection property.

Figure 25: Reflective lighting arrangement

- In addition, following international standards and concepts along with appropriate mannequins and creative arrangements can be displayed in interior sites, which enable stores to introduce their new fashions and key items in a more effective way.

Figure 26: Mannequins with creative arrangements

6. CONCLUSION

According to the outcome of the study, it is clear that in Sri Lanka females do shopping more than the male. 72% of the sample of 200 randomly picked customers at four stores were female and only 28 % were male. The age group of 72% of the respondents was between 25 – 44 years and majority was between 25-34 years of age. It is clear that young working adults do shopping than other age groups. In Sri Lanka children clothing is decided by the parents. For older people, mostly their children do the shopping. According to the study, it is clear that visual merchandising elements play a vital role in the retail business and it has a great impact on consumers' buying behaviour. The highly effective visual merchandising elements are window display, mannequins, colour combination, use of music and creative displays.

Under the recommendation, visual merchandising elements, adopted by international branded stores are indicated, hoping those elements will help the Sri Lankan retail stores improve their business.

REFERENCES

1. Saini, C. (2015). Visual Merchandising and Impulse Buying Behavior: A Case of Retail Industry. *International Journal of Advance Research in Science & Engineering*, Vol.4, Issue: 2, pp.621-627.

2. Kaur, A. (2013). Effects of Visual Merchandising on Buying Behavior of Customers in Chandigarh. *International Journals of Engineering Science and Innovative Technology*, Vol.2, Issue:3, pp.247-251.

3. Arjun, R. (2014). Visual merchandising in Retailing: Influencing Consumer Buying Behavior Towards Apparels with Special Reference to Pune City in India. *International Journal of Marketing and Technology*, Vol.4, Issue:5, pp.74-94.

4. Madhavi, S. (2013). Impact of Visual Merchandising on Consumer Behavior towards Women Apparel. *International Journal of Management Research and Business Strategy*, Vol.2, Issue: 4, pp.61-72.

5. Makhal, A.B (2015). The Importance of Visual Merchandising on Consumer Loyalty, A Study Conducted in Kolkata. *The International Journal of Business & Management,* Vol.3, Issue: 5, pp.195-202.

6. Bhatti, K. l. (2014). The Impact of Visual Merchandising on Consumer Impulse Buying Behavior. *Eurasian Journal of Business & Management*, Vol.2, Issue: 1, pp.24-35.

7. Tabassum, R., & Khan, I. (2015), Impact of Visual Merchandising on Consumer Buying Behavior: A Study on Retail Outlets. *International Journal of Scientific Research*, Volume: 4, Issue: 5, pp. 3 – 13.

8. Manali Khaniwale, April 2015. "Consumer Buying Behavior," *International Journal of Innovation and Scientific Research*, vol. 14, no. 2, pp. 278–286.

9. Matthysz, D. (2003). "Visual merchandising", *TTM5240: Apparel Merchandising* (pp. 23-34). Nwala, Nugegoda. The Open University of Sri Lanka.